The axial nucleon charge g_A (and its renormalization constant Z_A) using the point-split axial vector current operator on the lattice

Stanislav Kazmin
with Arwed Schiller and Holger Perlt

University Leipzig

25.11.2016

Content

Introduction – Basics

Why Lattice QCD?

- fundamental quantum field theory of quarks and gluons
- large energies: asymptotically free $\rightarrow$ perturbation theory
- small energies: coupling large $\rightarrow$ nonperturbative techniques

Basic steps towards lattice QCD

1. discretize Euclidean space-time by a hyper-cubic lattice Λ
   - lattice volume: $V = L^3 \times T$
   - lattice spacing: a
2. construct a discrete version of the QCD action
3. quantize QCD using Euclidean path integrals
4. calculate expectation values using Monte Carlo techniques

Fermion fields $\psi_f(x)^c_\alpha$ and $\bar{\psi}_f(x)^c_\alpha$

- live on lattice sites as $N_c \otimes N_d$ objects

Link variables $U_\mu(x)$

- link variables $U_\mu(x) \in \mathrm{SU}(3)$ as parallel gauge transporters from point x to a neighboring point $x + \hat{\mu}$ (Figure 1)
- connected to gauge fields $A_\mu(x)$ in the continuum by

$$U_\mu(x) = \exp(\mathrm{i}aA_\mu(x)) \tag{1}$$

Figure 1: link variables on the links between two sites

Wilson plaquette $U^{\square}(x)$

- closed loops of $U_\mu(x)$ are gauge invariant
- smallest closed loop is the Wilson plaquette

$$U^{\square}_{\mu\nu}(x) = U_\mu(x)\,U_\nu(x+\hat{\mu})\,U^{\dagger}_{\mu}(x+\hat{\nu})\,U^{\dagger}_{\nu}(x) \tag{2}$$

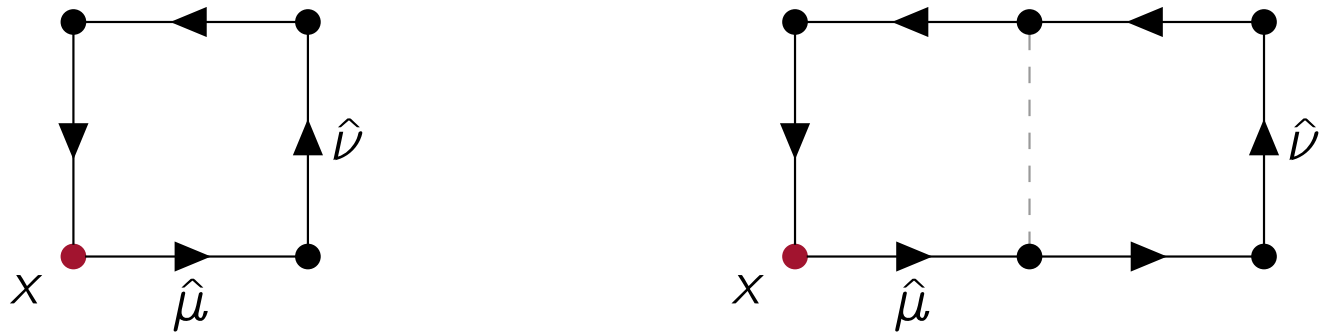

a plaquette $U^{\square}(x)$ b planar rectangle $R^{\square}_{\mu\nu}(x)$

Figure 2: schematic Wilson plaquette $U^{\square}(x)$ and planar rectangle $R^{\square}(x)$

Integration on lattice

$$\int \mathrm{d}^4 x \;\rightarrow \sum_{x \in \Lambda} \tag{3}$$

Parameters

- Inverse coupling $\beta = \frac{6}{g^2}$ (4)
- Hopping parameter $\kappa_f = \frac{1}{2(m_f + 4)}$ (5)
- work with $2 + 1$ flavors $\rightarrow$ two light quarks with isospin symmetry and the strange quark

Introduction – Improved QCD Action

- gauge fields are tree-level Symanzik improved
- quark fields are clover improved and contain the Wilson term
- $D_f(x, y)$ is the Dirac operator

$$S(U, \psi, \bar{\psi}) = S_F(U, \psi, \bar{\psi}) + S_G(U) \tag{6}$$

$$S_G(U) = \frac{\beta}{3} \int \mathrm{d}^4 x \left(C_0 \sum_{\mu<\nu} \mathrm{Re}\,\mathrm{Tr} \left(\mathbb{1} - U^{\square}_{\mu\nu}(x) \right) + C_1 \sum_{\mu<\nu} \mathrm{Re}\,\mathrm{Tr} \left(\mathbb{1} - R^{\square}_{\mu\nu}(x) \right) \right) \tag{7}$$

$$S_F(U, \psi, \bar{\psi}) = \sum_f \int \mathrm{d}^4 x \int \mathrm{d}^4 y \ \bar{\psi}_f(x) D_f(x, y) \psi_f(y) \tag{8}$$

Introduction – Improved QCD Action

Dirac Operator $D_f(x, y)$ with clover improvement

$$D_f(x,y) = \mathbb{1}\delta_{xy} - \kappa_f \sum_{\mu} (\mathbb{1} - \gamma_\mu) \left(U_\mu(x)\delta_{x+\hat{\mu},y} - U_{-\mu}(x)\delta_{x-\hat{\mu},y} \right) - c_{SW}\kappa_f \sum_{\mu,\nu} \frac{1}{2}\sigma_{\mu\nu}\hat{F}_{\mu\nu}(x)\delta_{xy} \tag{9}$$

- c_{SW} is the clover (or Sheikholeslami-Wohlert) coefficient
- $\hat{F}_{\mu\nu}(x)$ is the field strength tensor on lattice
- inverse Dirac Operator is the quark propagator $S(x, y)$

$$S(x,y) = D^{-1}(x,y) = \langle \psi(x)\,\bar{\psi}(y) \rangle_F \tag{10}$$

- the quark propagates from point y to point x

Expectation value of operator $\mathcal{O}$

- path integral formalism as in continuum

$$\langle \mathcal{O} \rangle = \frac{1}{\mathcal{Z}} \int \mathcal{D}U \, \mathcal{D}\psi \, \mathcal{D}\bar{\psi} \, \mathcal{O}(U, \psi, \bar{\psi}) \, e^{-S(U,\psi,\bar{\psi})} \tag{11}$$

- Grassmann numbers (anti-commuting numbers) allow to integrate out the fermionic part
- fermion determinant $\det D_f(x, y)$ as an effective action

$$\langle \mathcal{O} \rangle = \frac{1}{\mathcal{Z}} \int \mathcal{D}U \, \tilde{\mathcal{O}}(S_f, U) \, e^{-\tilde{S}(U)} \tag{12}$$

$$\tilde{S}(U) = S_G(U) + S_F^{\text{eff}}(U) \tag{13}$$

$$S_F^{\text{eff}}(U) = -\sum_f \operatorname{Tr} \ln D_f \tag{14}$$

Configuration ensemble

configuration $\mathcal{U}_i$ is a set of link variables

$$\mathcal{U}_i = \{U_\mu(x) \mid x \in \Lambda,\ \mu = 1, \ldots, 4\} \tag{15}$$

ensemble $\mathcal{U}$ is a set of configurations $\mathcal{U}_i$

- generate ensemble $\mathcal{U}$ with a Hybrid Monte Carlo algorithm
- configurations $\mathcal{U}_i$ distributed according to the weight

$$W = \frac{1}{\mathcal{Z}}\, e^{-\tilde{S}(U)} \tag{16}$$

- use importance sampling to obtain expectation values $\langle \mathcal{O} \rangle$ and errors $\sigma(\mathcal{O})$

Introduction – Analysis Steps

1. configuration generation
   - used configurations produced by the QCDSF collaboration
2. measurements
   - performed at the HRLN supercomputing system
   - used the Chroma C++ package
   - used self-written Chroma module for the vertex function calculation from the point-split axial current operator
3. data analysis
   - performed in Leipzig with self-written Julia code

Content

Nucleon Axial Charge g_A – Introduction

- axial vector current operator $A_\mu = \bar{\psi}(x)\gamma_\mu\gamma_5\psi(x)$
- nucleon matrix element $\langle N(p', s')|A_\mu|\bar{N}(p, s)\rangle$
  - proportional to the axial form factor $G_A(q^2)$
  - proportional to nucleon beta decay rate
- axial charge is defined by $g_A = G_A(q^2 = 0)$
- g_A is a benchmark quantity in lattice QCD
- current lattice measurements usually underestimate the experimental value $g_A^{\text{exp}} = 1.2723(23)$

Nucleon Axial Charge g_A – Introduction

Axial vector current operator A_μ on the lattice

- local operator $A_\mu^{\text{loc}}(x)$ or point-split operator $A_\mu^{\text{ps}}(x)$

$$A_\mu^{\text{loc}}(x) = A_\mu = \bar{\psi}(x)\gamma_\mu\gamma_5\psi(x) \tag{17}$$

$$A_\mu^{\text{ps}}(x) = \frac{1}{2}\left(\bar{\psi}(x)\gamma_\mu\gamma_5 U_\mu(x)\psi(x+\hat{\mu}) + \bar{\psi}(x+\hat{\mu})\gamma_\mu\gamma_5 U_\mu^\dagger(x)\psi(x)\right) \tag{18}$$

Motivation for A_μ^{ps}:

- at comparable pion masses estimates, that are closer to the experimental value than for A_μ^{loc}
- renormalization constant is closer to one

Nucleon Axial Charge g_A – Introduction

Ratio of correlation functions can be used to determine g_A

$$R(t;\tau) = \frac{G_3(t;\tau)}{G_2(t)} = g_A \tag{19}$$

Correlation functions

$$G_2(t) = \sum_{\boldsymbol{x}} e^{-i\boldsymbol{p}\boldsymbol{x}}\, \Gamma^{(2)}_{\beta\alpha} \langle N_\alpha(x) \bar{N}_\beta(0) \rangle \tag{20}$$

$$G_3(t;\tau) = \sum_{\boldsymbol{x},\boldsymbol{y}} e^{-i\boldsymbol{p}\boldsymbol{x}} e^{-i\boldsymbol{p}'(\boldsymbol{x}-\boldsymbol{y})}\, \Gamma^{(3)}_{\beta\alpha} \langle N_\alpha(x) \mathcal{O}(y) \bar{N}_\beta(0) \rangle \tag{21}$$

with the nucleon interpolators N and projectors Γ

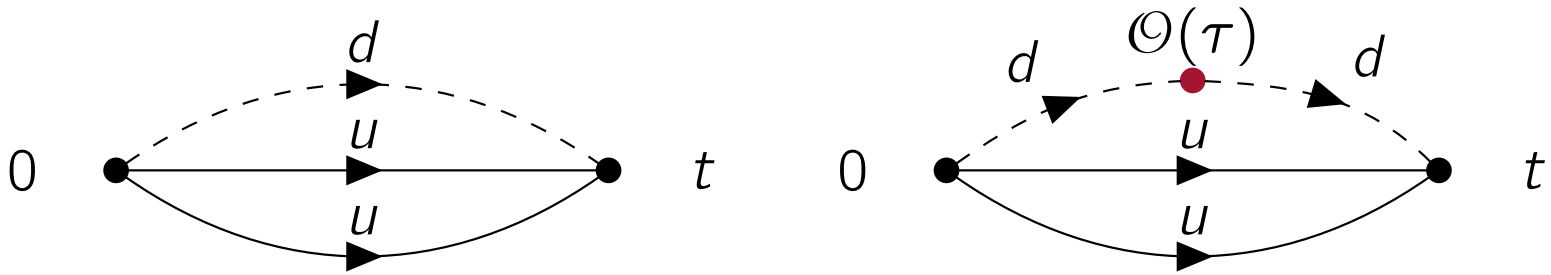

Figure 3: Two-point and three-point function of a nucleon

Nucleon Axial Charge g_A – Measurements

Performed measurements

$L^3 \times T$	β	a / fm	t, m_π / MeV	meas.
$32^3 \times 64$	5.50	0.0740	$t = 13, 15, 17, 19, 21$ $m_\pi = 465$	≈ 2600
$48^3 \times 96$	5.80	0.0558	$t = 15, 17, 19, 21, 23$ $m_\pi = 427$	≈ 600

- varied separation time t between source and sink at symmetric point ($\kappa_l = \kappa_s = \kappa$)
- got curves $g_A(\tau)$ for each t and $\bar{g}_A$ as the mean value in the range $0 \ll \tau \ll t$

Nucleon Axial Charge g_A – Measurements

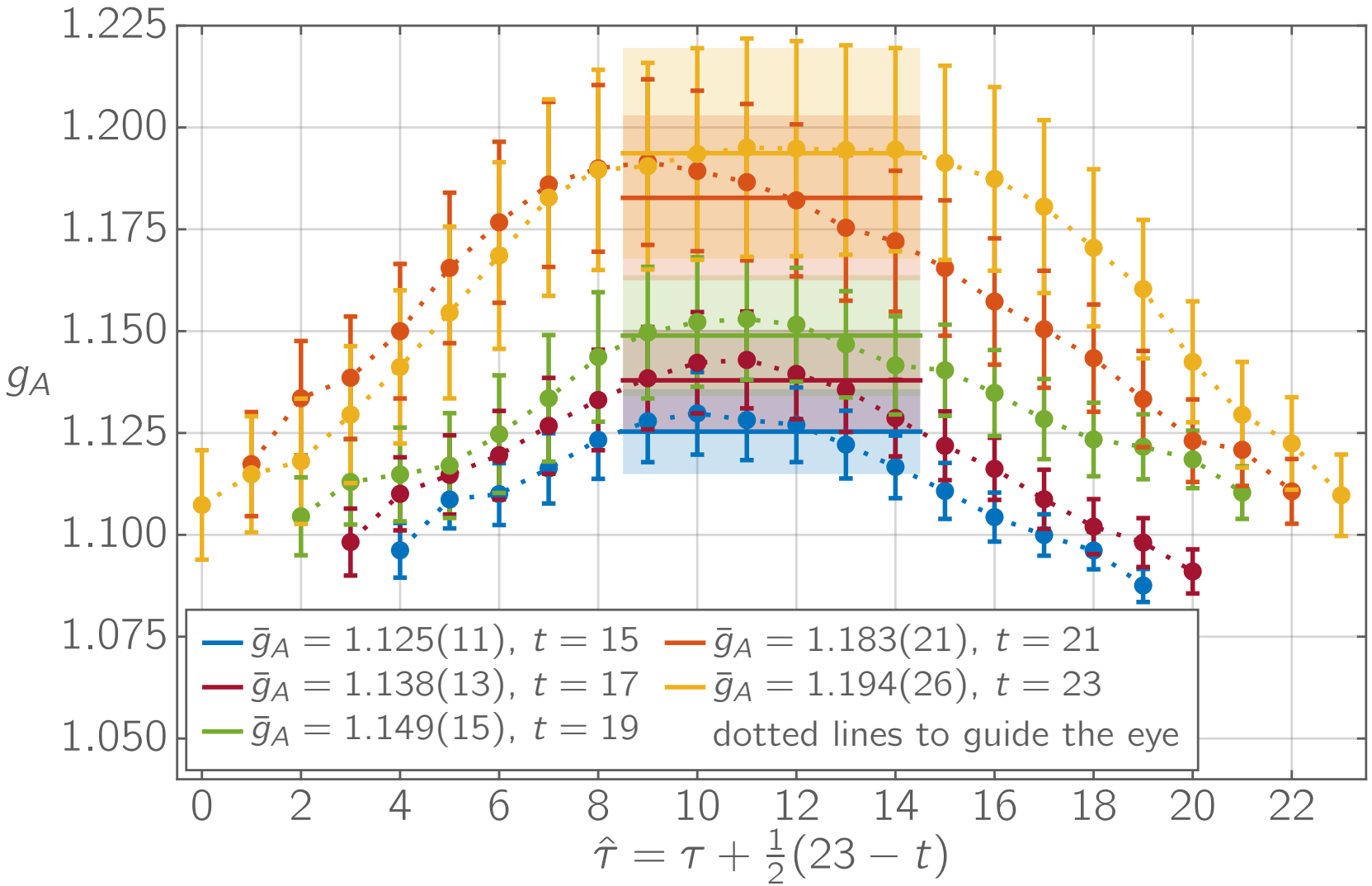

Figure 4: $\bar{g}_A$ for different separation times t for $\beta = 5.80$

Nucleon Axial Charge g_A – Results

Excited states contribution

- g_A depends on separation time t
- for small and large t values the contribution is large
- systematically analyzed with two different methods
  1. Summation method
  2. Global fit method

Global fit method

1. from G_2 obtain the ground state mass and two excited state masses M_i with a symmetric fit ansatz
2. insert the obtained masses into a global fit function which involves all $g_A(t, \tau)$ values

Nucleon Axial Charge g_A – Results

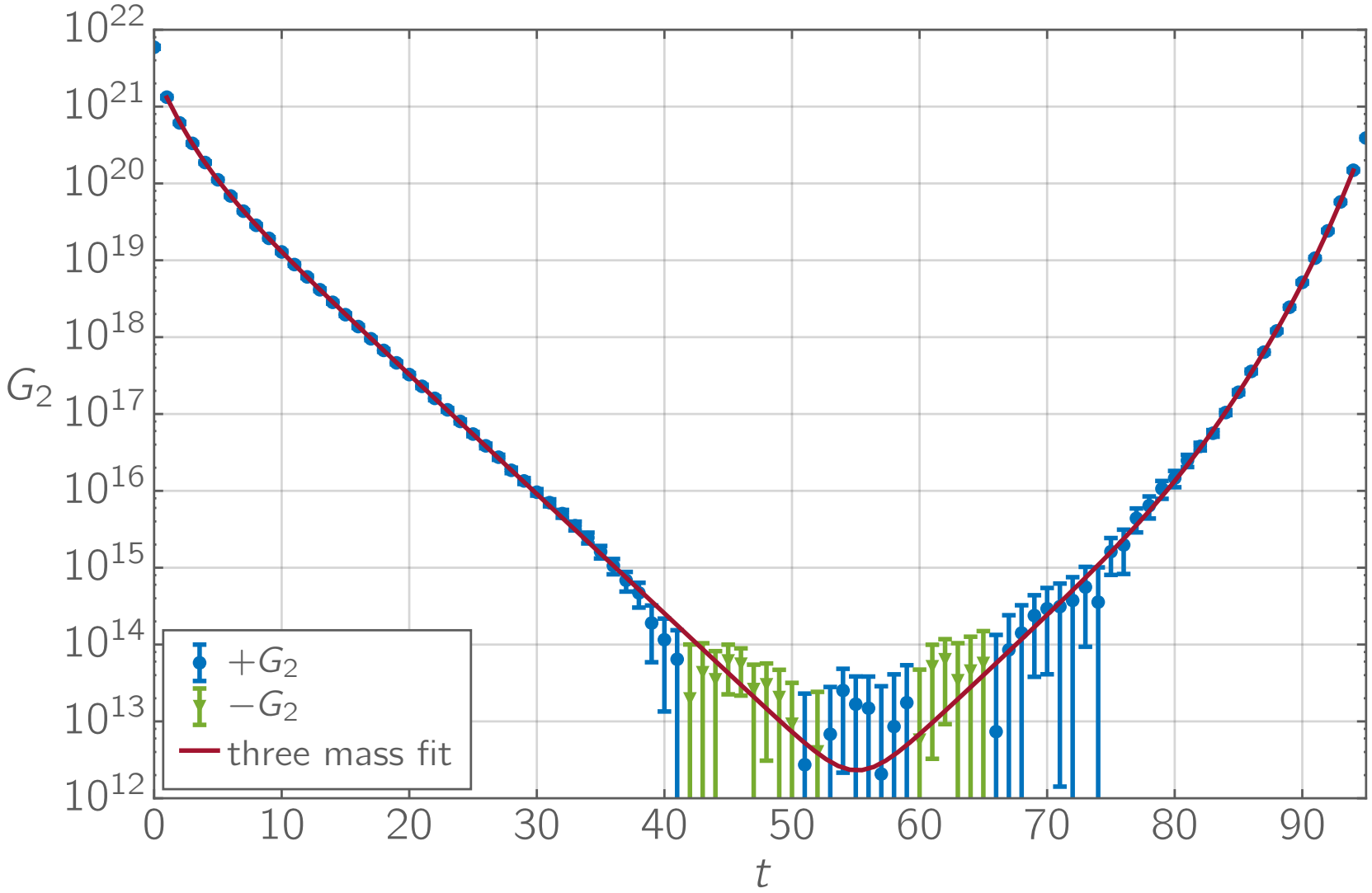

Figure 5: G_2 three mass fit for $\beta = 5.80$

Nucleon Axial Charge g_A – Results

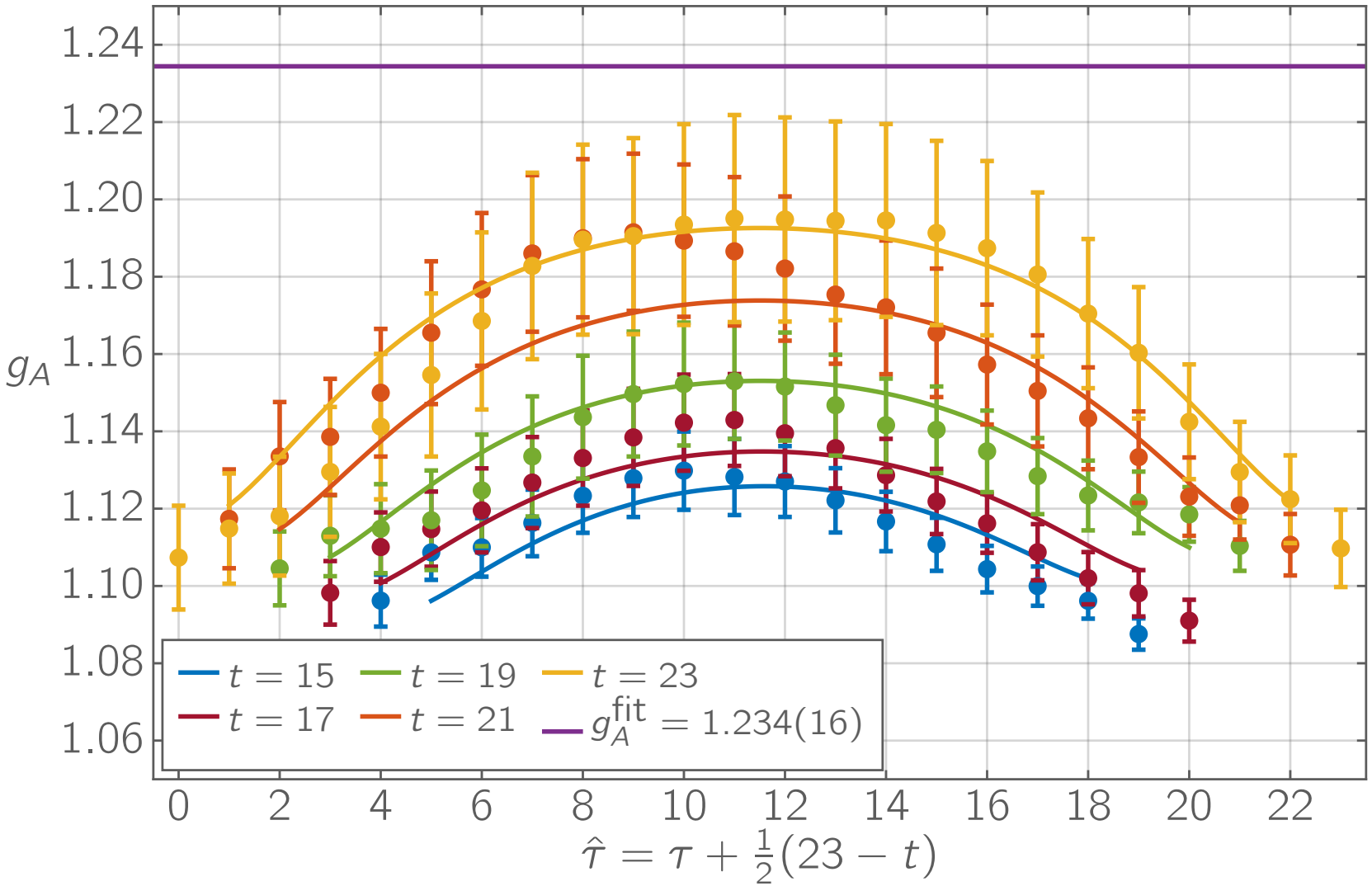

Figure 6: Global fit method result for $\beta = 5.80$

Content

Summary and Outlook

- excited states contributions can be treated with global fit method
- higher g_A estimate than with the local operator for comparable pion masses ($\beta = 5.50$, renormalized)

$$g_A^{\text{ps}} = 1.224(11) \quad g_A^{\text{loc}} = 1.1203(95) \quad g_A^{\text{exp}} = 1.2723(23)$$

- Renormalization constant closer to one ($\beta = 5.50$)

$$Z_A^{\overline{\text{MS}}} = 1.0212(12)(47) \quad Z_A^{\overline{\text{MS}},\text{loc}} = 0.8728(06)(27)$$

Outlook:

- Feynman-Hellmann approach could improve the measurement as it does not involve three-point correlation functions
- extrapolate g_A to the physical point
- measure Z_A for $\beta = 5.80$ (expect to be even closer to one)

Thank You for Your Attention!

Stanislav Kazmin
with Arwed Schiller and Holger Perlt

University Leipzig

25.11.2016

Sources

[1] C. Gattringer and C. B. Lang, *Quantum chromodynamics on the lattice: an introductory presentation*, Lecture notes in physics 788 (Springer, Heidelberg ; New York, 2010), 343 pp., ISBN: 978-3-642-01849-7.

[2] B. Jäger, "Hadronic matrix elements in lattice QCD", (May 14, 2014), http://ubm.opus.hbz-nrw.de/volltexte/2014/3741/.

[3] H. J. Rothe, *Lattice Gauge Theories: An Introduction*, (World Scientific, Jan. 29, 1992), 397 pp., ISBN: 978-981-4602-30-3.

[4] B. Sheikholeslami and R. Wohlert, "Improved continuum limit lattice action for QCD with wilson fermions", Nuclear Physics B **259**, 572–596 (1985).

Sources

[5] H. Matsufuru, *Lattice QCD simulations with clover quarks*, Apr. 2012, http://suchix.kek.jp/hideo_matsufuru/Research/Docs/Bridge/Clover_HMC/note_cloverHMC_1.3.1.pdf.

[6] R. Horsley, "The Hadronic Structure of Matter – a Lattice approach", (Institut für Physik, Humboldt-Universität zu Berlin, Jan. 18, 2000), 152 pp.

[7] H. Matsufuru, *Introduction to lattice QCD simulations*, Sept. 7, 2007, http://www.rcnp.osaka-u.ac.jp/%5C%0020%5C%003c%5C%0020matufuru/.

[8] *The Julia Language (NumFocus project)*, (2016) http://julialang.org/.

[9] *HLRN*, https://www.hlrn.de/home/view/Service.

Sources

[10] R. G. Edwards and B. Joó, "The Chroma Software System for Lattice QCD", Nuclear Physics B - Proceedings Supplements **140**, 832–834 (2005), arXiv:hep-lat/0409003.

[11] J. Zanotti, "Hadron Structure", Seattle, USA, Aug. 6–24, 2012, http://www.int.washington.edu/PROGRAMS/12-2c/week3/.

[12] M. E. Peskin and D. V. Schroeder, *An introduction to quantum field theory*, (Addison-Wesley Pub. Co, Reading, Mass, 1995), 842 pp., ISBN: 978-0-201-50397-5.

[13] K. A. Olive and Particle Data Group, "Review of Particle Physics", Chinese Physics C **38**, 090001 (2014).

Sources

[14] R. Horsley, Y. Nakamura, H. Perlt, P. E. L. Rakow, G. Schierholz, A. Schiller, and J. M. Zanotti, "Improving the lattice axial vector current", Proceedings, 33rd International Symposium on Lattice Field Theory (Lattice 2015) (2015).

[15] C. Alexandrou, R. Baron, M. Brinet, J. Carbonell, V. Drach, P.-A. Harraud, T. Korzec, and G. Koutsou, "Nucleon form factors with dynamical twisted mass fermions", (2008), arXiv:0811.0724 [hep-lat].

[16] D. B. Leinweber, R. M. Woloshyn, and T. Draper, "Electromagnetic structure of octet baryons", Physical Review D **43**, 1659–1678 (1991).

Sources

[17] G. von Hippel, J. Hua, B. Jäger, H. B. Meyer, T. D. Rae, and H. Wittig, "Fitting strategies to extract the axial charge of the nucleon from lattice QCD", PoS **LATTICE2013**, 446 (2014).

[18] B. Jäger, T. D. Rae, S. Capitani, M. Della Morte, D. Djukanovic, G. von Hippel, B. Knippschild, H. B. Meyer, and H. Wittig, "A high-statistics study of the nucleon EM form factors, axial charge and quark momentum fraction", (2013), arXiv:1311.5804 [hep-lat].

[19] S. Collins, "Proceedings, 34th International Symposium on Lattice Field Theory (Lattice 2016)", PoS **LATTICE2016** (2016).

Backup – Renormalization Constant Z_A

- observables measured with lattice QCD must be renormalized to compare them to real physical values
- many observables diverge in the limit $a \to 0$

Necessary steps for a lattice renormalization scheme

1. remove the ultraviolet divergence in the observables
   - perturbatively: in general bad convergence
   - nonperturbatively: used RI'-MOM scheme (regularization independent momentum subtraction)
2. match a convenient continuum scheme
   - common choice: $\overline{\text{MS}}$ scheme (minimal subtraction)
   - typical comparison scale $\mu_R = 2\,\text{GeV}$

Backup – Renormalization Constant Z_A

Axial current renormalization constant Z_A

- $Z_A = 1$ for chirally symmetric actions and conserved current
- stays finite in the continuum limit $a \to 0$

Calculation steps

1. calculate $Z_A^{\mathrm{RI'}}(\hat{p}^2; \kappa_i)$ in RI'-MOM scheme for quark masses along the symmetric line $\kappa_l = \kappa_s = \kappa$
2. calculate $Z_A^{\mathrm{RI'}}(\hat{p}^2; \kappa_{\mathrm{cr}}^{\mathrm{sym}})$ by taking the chiral limit $m \to 0$ of $Z_A^{\mathrm{RI'}}(\hat{p}^2; \kappa_i)$ at each $\hat{p}^2$
3. rescale the $Z_A^{\mathrm{RI'}}(\hat{p}^2; \kappa_{\mathrm{cr}}^{\mathrm{sym}})$ with a scale function $R_{RI' \to \overline{\mathrm{MS}}}(\hat{p}^2)$ which lead to $Z_A^{\overline{\mathrm{MS}}}(\hat{p}^2)$
4. analyze the $Z_A^{\overline{\mathrm{MS}}}(\hat{p}^2)$ curve and obtain the final $Z_A^{\overline{\mathrm{MS}}}$

Backup – Renormalization Constant Z_A

RI'-MOM scheme

- applicable in a scale window

$$\Lambda^2_{QCD} \ll \mu^2_R \ll \frac{1}{a^2} \tag{22}$$

- needs gauge fixed configurations (used Landau gauge)

- ideally, $Z_A^{\overline{\text{MS}}}$ is scale independent but due to lattice artifacts we see a dependence
- lattice artifacts considered to be small: linear fit ansatz
- choice of the fit range $\hat{p}^2_{\text{min}} \ldots \hat{p}^2_{\text{max}}$ leads to systematic error

Backup – Measurements

Performed measurements

κ	0.12090	0.12092	0.12095	0.12099	0.121021
m_π / MeV	465	439	402	343	290
cfg.	18	9	18	10	9

- $\beta = 5.50$, lattice size: $32^3 \times 64$, $a = 0.0740\,\mathrm{fm}$
- diagonal momenta in the range $0 \leq \hat{p}^2 \leq 10$
- total number of momenta increased to 32 by using twisted boundary conditions

$$\hat{p}_i = \frac{2\pi}{L}(n_i + \theta_i)\,, \quad \hat{p}_4 = \frac{2\pi}{T}(n_4 + \theta_4 + \frac{1}{2}) \qquad (23)$$

Backup – Results

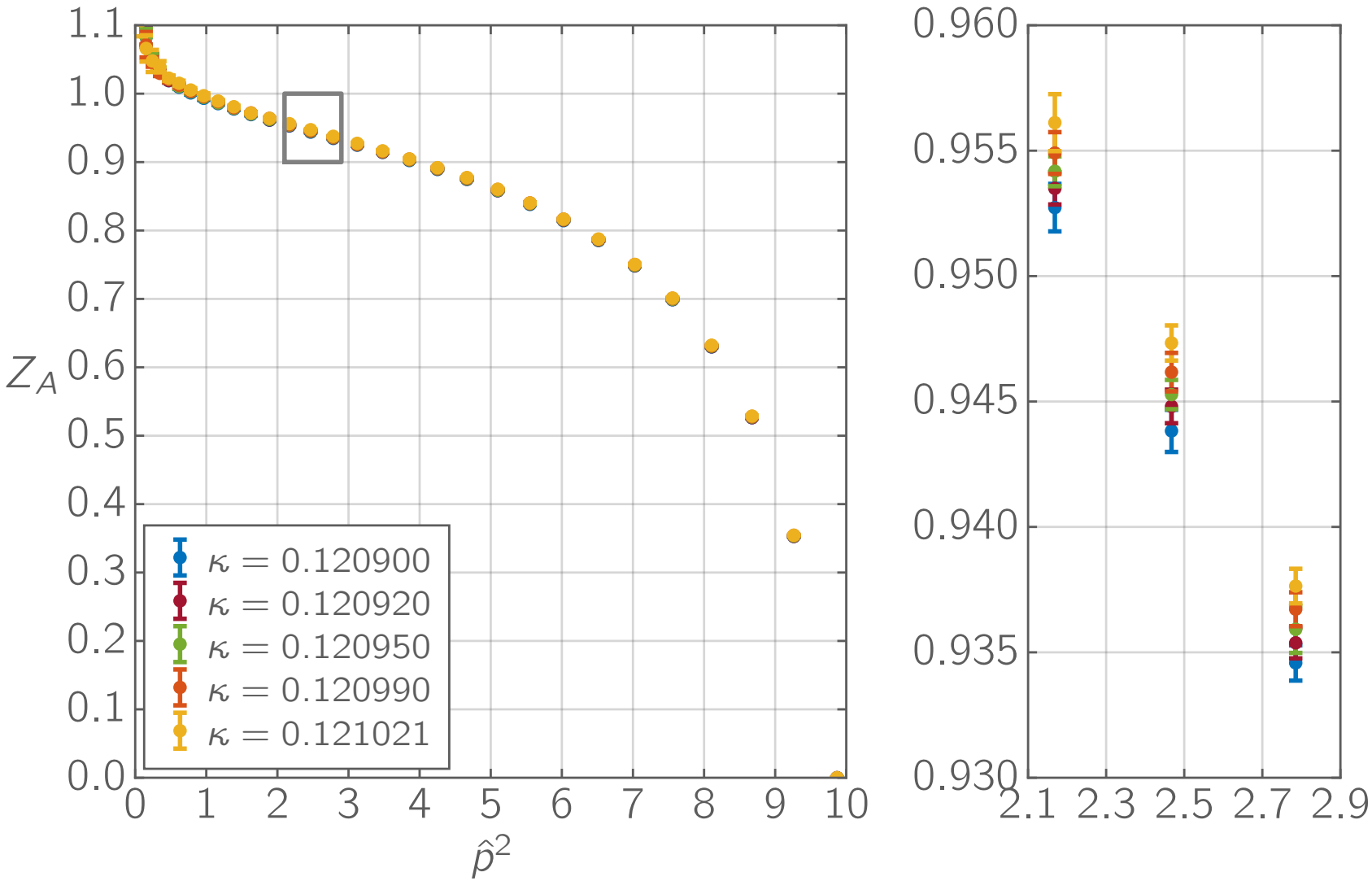

Figure 7: $Z_A(\hat{p}^2)$ for different kappa values (zoomed region highlighted)

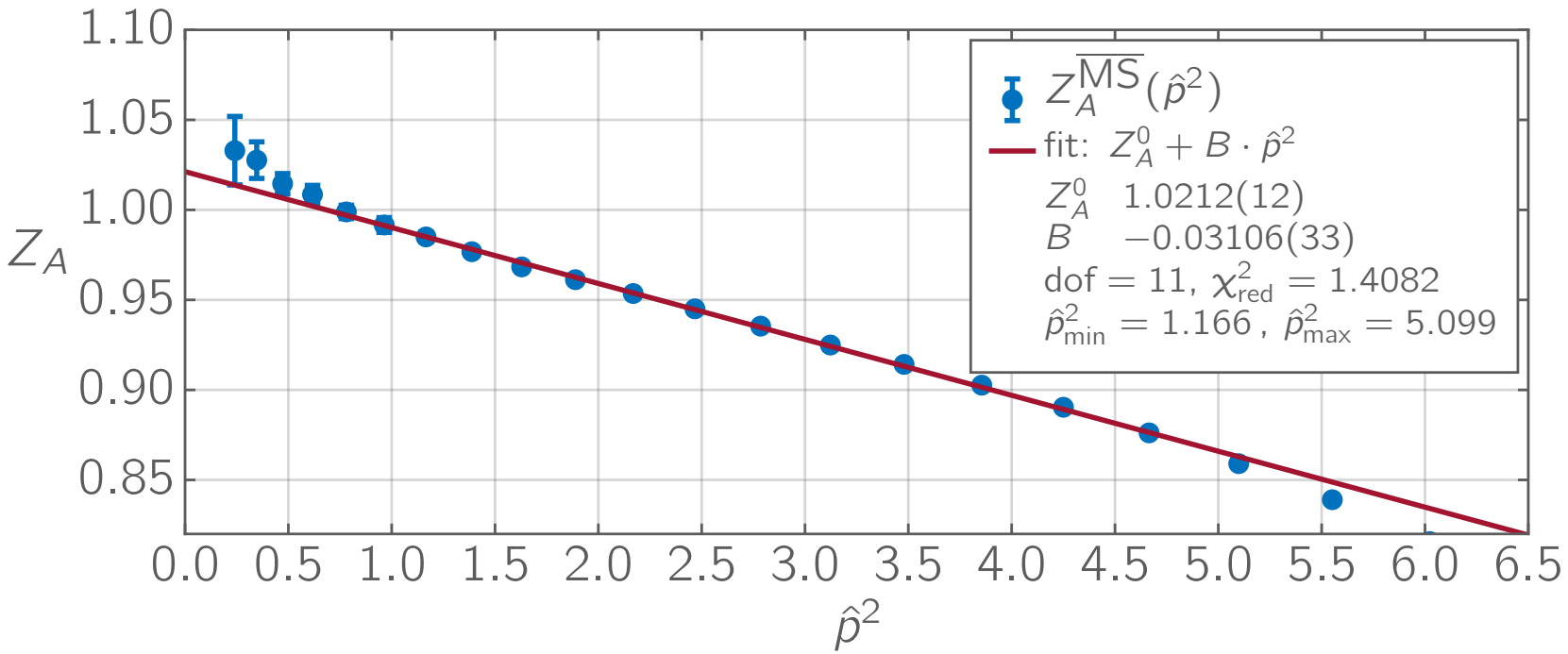

Figure 8: $Z_A^{\overline{\text{MS}}}(\hat{p}^2)$ curve and linear fit

Renormalization constant Z_A result for $\beta = 5.50$

$$Z_A^{\overline{\text{MS}}} = 1.0212(12)(47)$$

Backup – Sequential Propagator Technique

a Calculate the ordinary quark propagator $S^{\psi}(\boldsymbol{x}, t; 0)$

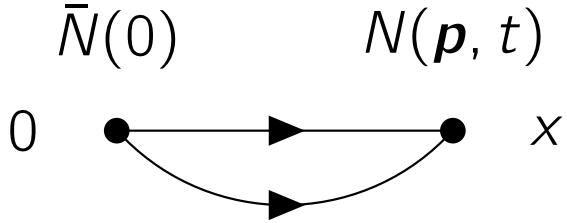

b Construct the sequential source $S^{\psi}_{\text{seq}}(\boldsymbol{x}, t; 0; \boldsymbol{p})$

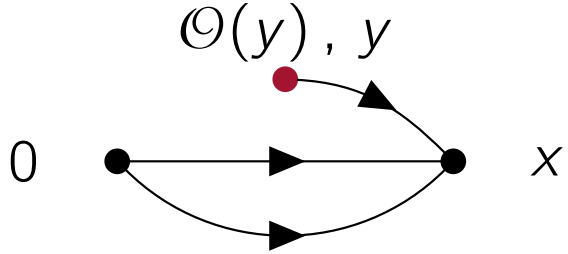

c Compute the sequential propagator $\Sigma^{\psi}(0; \boldsymbol{y}, \tau; \boldsymbol{p}, t)$ with a fermion matrix inversion and insert the operator $\mathcal{O}$

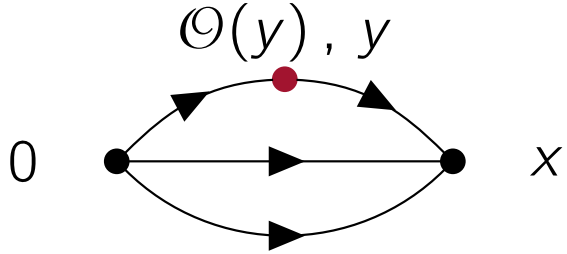

d Complete the correlation function with the ordinary quark propagator $S^{\psi}(\boldsymbol{y}, \tau; 0)$

Figure 9: Sequential propagator technique

Backup – Sequential Propagator Technique

Ratio of correlation functions can be used to determine g_A

$$R(t;\tau;A_\mu;\Gamma_\mu^{(3)}) = \frac{\frac{1}{3}\sum_{\mu=1}^{3} \mathrm{Im}\, G_3^{u-d}(t;\tau;A_\mu;\Gamma_\mu^{(3)})}{\mathrm{Re}\, G_2(t;\Gamma_\mu^{(2)})} = g_A \quad (24)$$

- polarized projector for the three-point function

$$\Gamma_\mu^{(3)} = \frac{1}{2}(\mathbb{1} + \gamma_4)\mathrm{i}\gamma_5\gamma_\mu \quad (25)$$

- unpolarized projector for the two-point function

$$\Gamma_\mu^{(2)} = \frac{1}{2}(\mathbb{1} + \gamma_4) \quad (26)$$

Backup – Sequential Propagator Technique

Two-point correlation function

$$G_2(\boldsymbol{p}, t) = \int \mathrm{d}^3x \; e^{-\mathrm{i}\boldsymbol{p}\boldsymbol{x}} \epsilon_{abc} \, \epsilon_{a'b'c'}$$
$$\Big\langle \mathrm{Tr}\left(\Gamma^{(2)} S^u(x,0)^{aa'}\right) \mathrm{Tr}\left(\tilde{S}^d(x,0)^{bb'} S^u(x,0)^{cc'}\right)$$
$$+ \mathrm{Tr}\left(\Gamma^{(2)} S^u(x,0)^{aa'} \tilde{S}^d(x,0)^{bb'} S^u(x,0)^{cc'}\right) \Big\rangle \quad (27)$$

- the tilde operation is defined by

$$\tilde{S} = \left(C\gamma_5 \, S \, C\gamma_5\right)^T \quad (28)$$

- only one-to-all propagators
- low effort calculation

Backup – Sequential Propagator Technique

Three-point correlation function

$$G_3^{\psi}(\boldsymbol{p}, t; \boldsymbol{p}', \tau; \mathcal{O}; \Gamma^{(3)})$$
$$= \int \mathrm{d}^3 y \; e^{\mathrm{i}\boldsymbol{q}\boldsymbol{y}} \left\langle \mathrm{Tr}\left[\Sigma^{\psi}(0; \boldsymbol{y}, \tau; \boldsymbol{p}, t)\, \mathcal{O}^{\psi}(\boldsymbol{y}, \tau)\, S^{\psi}(\boldsymbol{y}, \tau; 0)\right]\right\rangle \quad (29)$$

- sequential propagator Σ^{ψ}

$$\Sigma^{\psi}(0; \boldsymbol{y}, \tau; \boldsymbol{p}, t) = \int \mathrm{d}^3 x \; S^{\psi}_{\mathrm{seq}}(\boldsymbol{x}, t; 0; \boldsymbol{p}) S(\boldsymbol{x}, t; \boldsymbol{y}, \tau) \quad (30)$$

- in sequential sources S^{ψ}_{seq} skip disconnected terms as they cancel each other in

$$G_3^{u-d} = G_3^{u} - G_3^{d} \quad (31)$$

Backup – Sequential Propagator Technique

Sequential sources S^{ψ}_{seq} for the nucleon

$$
\begin{aligned}
S^{d}_{\text{seq}}(\boldsymbol{x}, t; 0; \boldsymbol{p})^{a'a} &= e^{-\mathrm{i}\boldsymbol{p}\boldsymbol{x}} \epsilon_{abc}\, \epsilon_{a'b'c'} \\
&\quad \times \Big[\tilde{S}^{u}(\boldsymbol{x}, t; 0)^{bb'} \tilde{\Gamma}^{(3)} \tilde{S}^{u}(\boldsymbol{x}, t; 0)^{cc'} \\
&\quad + \mathrm{Tr}\left(\Gamma^{(3)} S^{u}(\boldsymbol{x}, t; 0)^{bb'} S^{u}(\boldsymbol{x}, t; 0)^{cc'} \right) \Big] \qquad (32) \\
S^{u}_{\text{seq}}(\boldsymbol{x}, t; 0; \boldsymbol{p})^{a'a} &= e^{-\mathrm{i}\boldsymbol{p}\boldsymbol{x}} \epsilon_{abc}\, \epsilon_{a'b'c'} \\
&\quad \times \Big[\tilde{S}^{d}(\boldsymbol{x}, t; 0)^{bb'} \tilde{S}^{u}(\boldsymbol{x}, t; 0)^{cc'} \Gamma^{(3)} \\
&\quad + \mathrm{Tr}\left(\tilde{S}^{d}(\boldsymbol{x}, t; 0)^{bb'} S^{u}(\boldsymbol{x}, t; 0)^{cc'} \right) \Gamma^{(3)} \\
&\quad + \Gamma^{(3)} \tilde{S}^{u}(\boldsymbol{x}, t; 0)^{bb'} \tilde{S}^{d}(\boldsymbol{x}, t; 0)^{cc'} \\
&\quad + \mathrm{Tr}\left(\Gamma^{(3)} S^{u}(\boldsymbol{x}, t; 0)^{bb'} \tilde{S}^{u}(\boldsymbol{x}, t; 0)^{cc'} \right) \Big] \qquad (33)
\end{aligned}
$$

Backup – Sequential Propagator Technique

$\bar{g}_A(t = 13)$ quark mass dependence

- no mass dependence measured (in the given error range)
- compared only one separation time $t = 13$

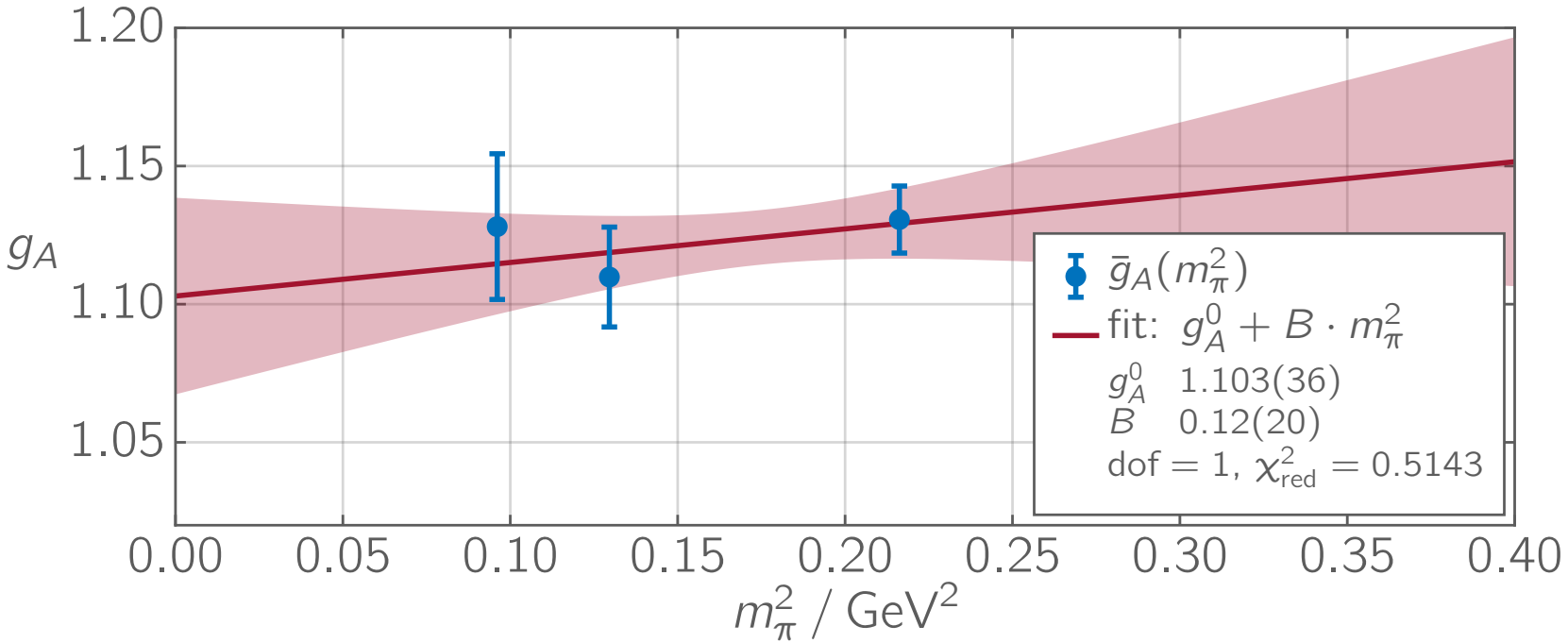

Figure 10: $\bar{g}_A$ for different quark masses

Backup – Plateau results for $\beta = 5.80$

Plateau values $\bar{g}_A$ for $\beta = 5.50$ and $\beta = 5.80$

- chosen symmetrical time range $\tau_{\text{min}} \ldots \tau_{\text{max}}$
- to remove contributions from excited states one has to fulfill

$$0 \ll \tau \ll t$$

- chosen the range according to this condition and to the good fit condition $\chi^2_{\text{red}} \approx 1$
- $\bar{g}_A$ is the mean value in the τ range

Backup – Plateau results for $\beta = 5.80$

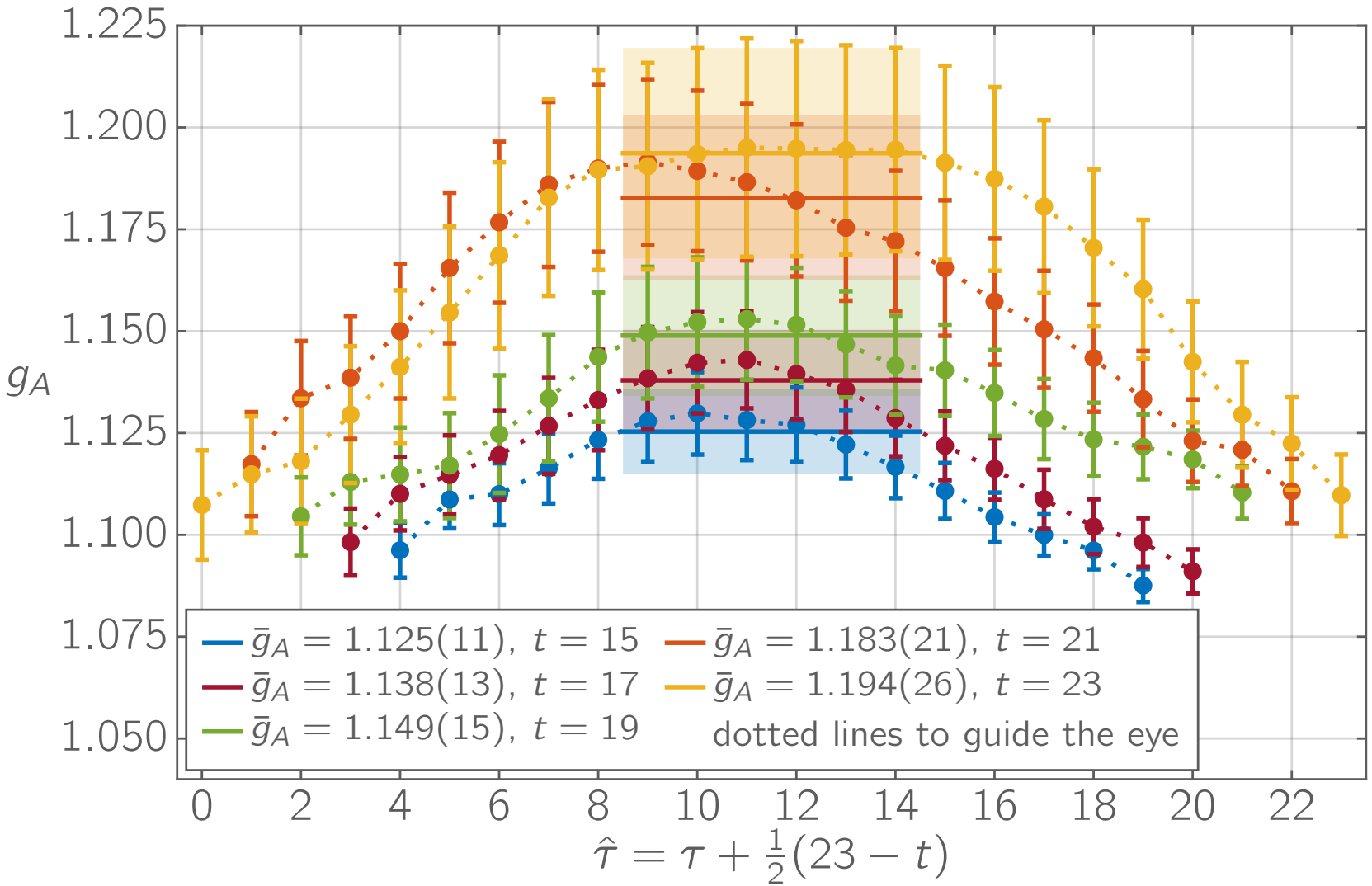

Figure 11: $\bar{g}_A$ for different separation times t for $\beta = 5.80$

Backup – Results for $\beta = 5.50$

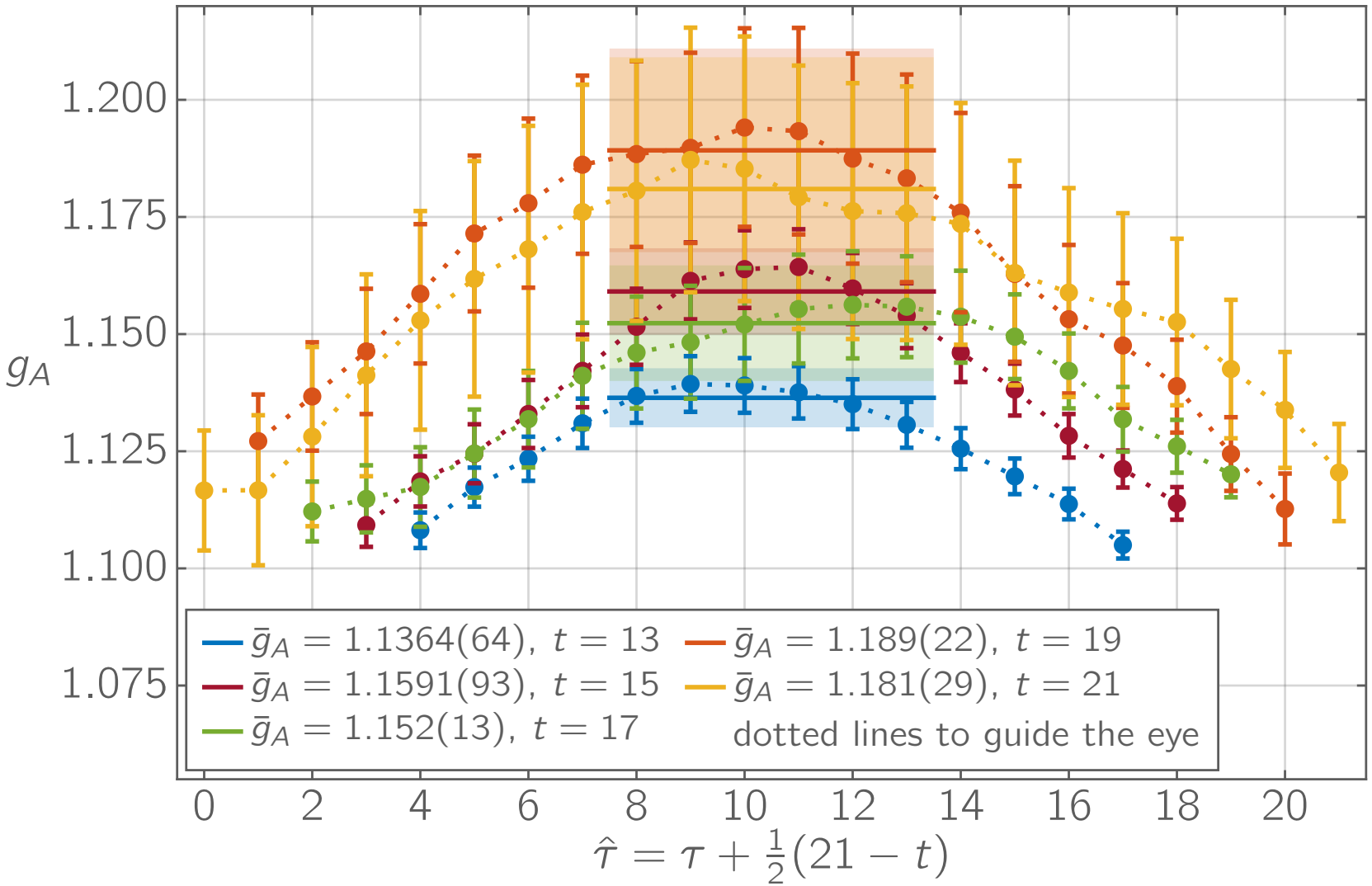

Figure 12: $\bar{g}_A$ for different separation times t for $\beta = 5.50$

Backup – Results for $\beta = 5.50$

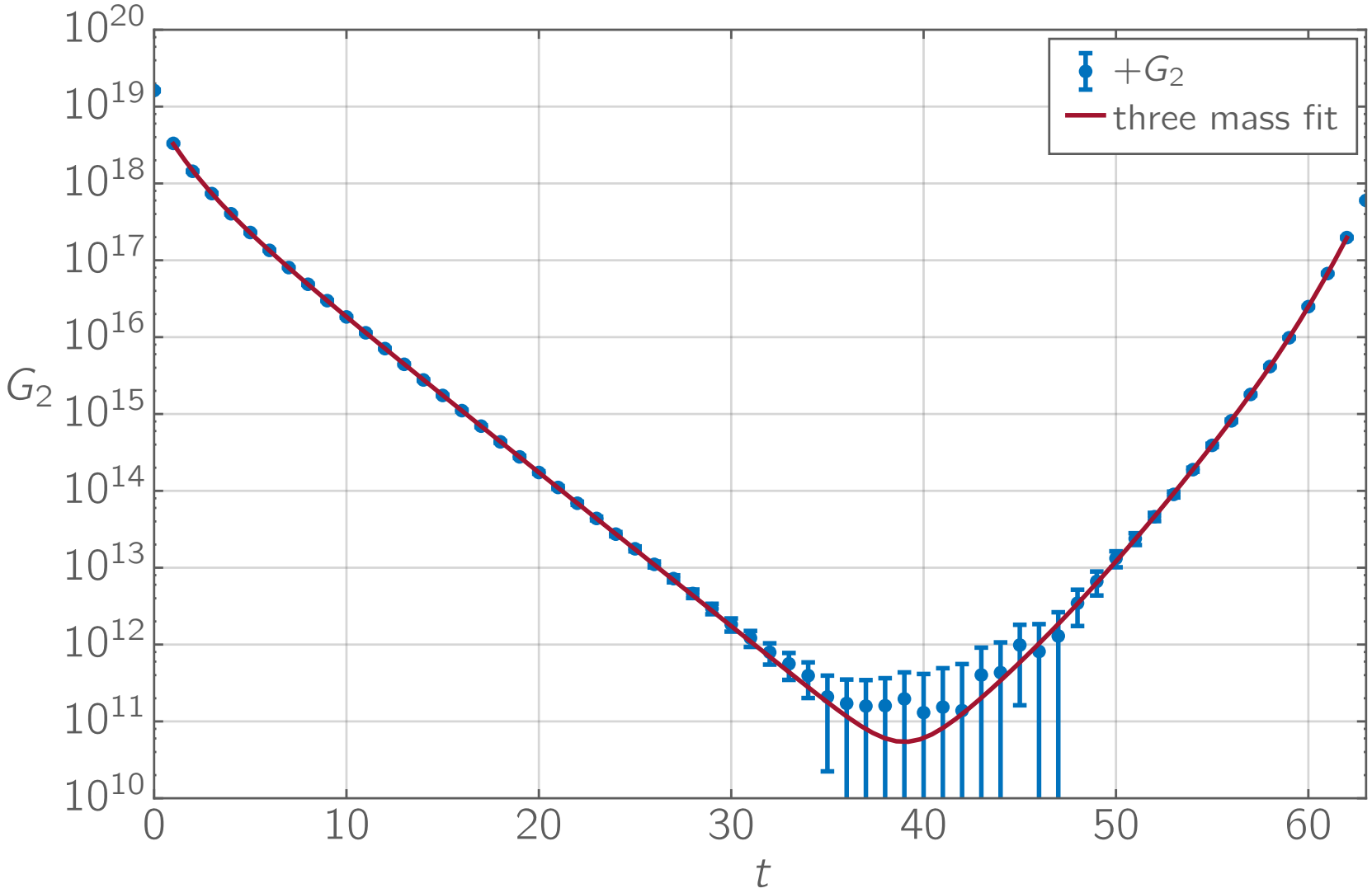

Figure 13: G_2 three mass fit for $\beta = 5.50$

Backup – Results for $\beta = 5.50$

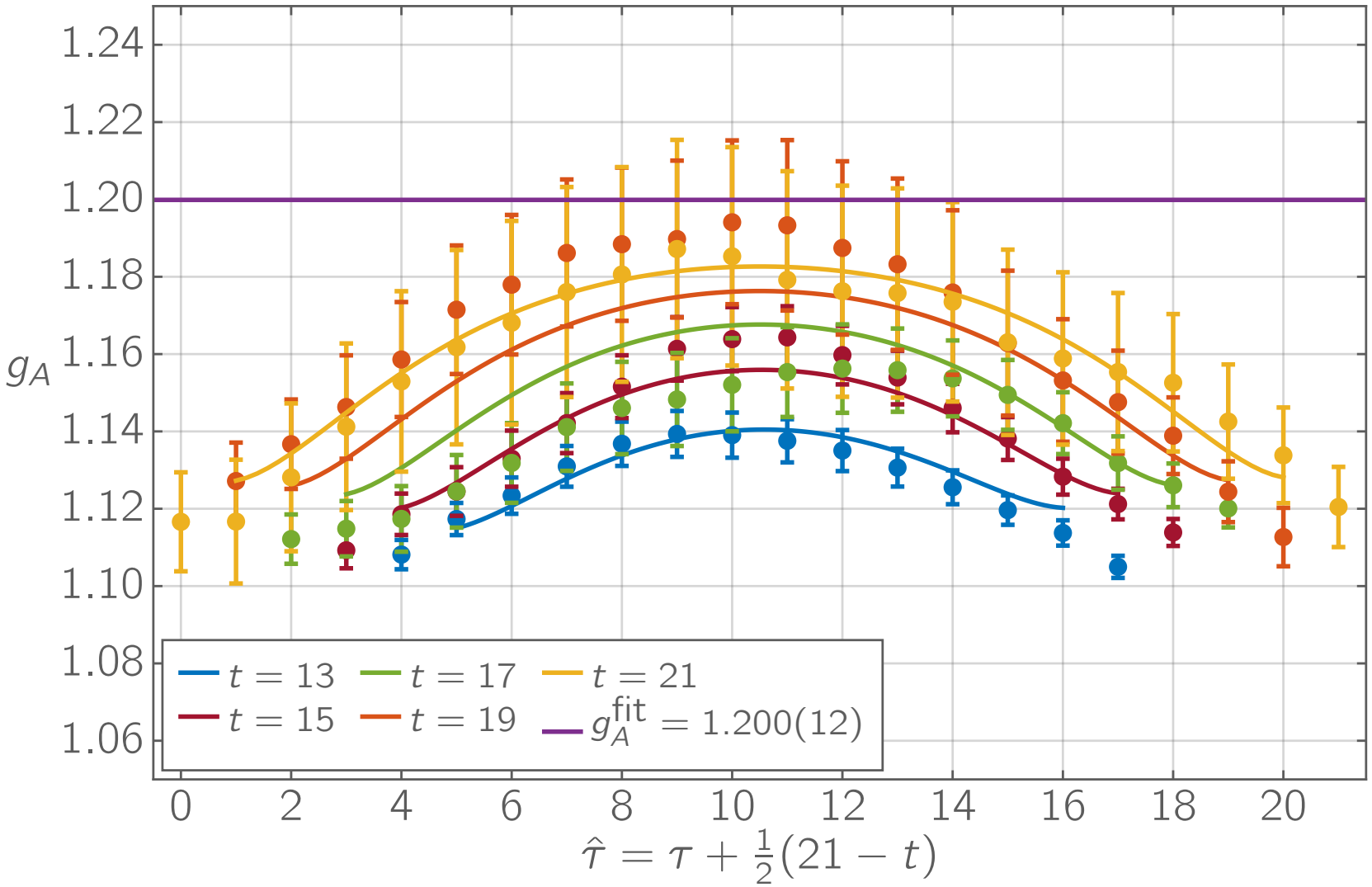

Figure 14: Global fit method result for $\beta = 5.50$

Summation method

- ansatz for the ratio (Δ is the energy gap between ground state and first excited state)

$$R(\tau, t) = g_A + C_1 e^{-\Delta \cdot \tau} + C_2 e^{-\Delta \cdot (t-\tau)} + C_3 e^{-\Delta \cdot t} + \dots \quad (34)$$

- sum over all ratio values $R(\tau, t)$ for each t (with cut t_c)

$$S(t) = \sum_{\tau=t_c}^{t-t_c} R(\tau, t) \quad (35)$$

$$S(t) \overset{t\to\infty}{\longrightarrow} S(t) = g_A^{\text{sum}}(t + 1 - 2t_c) + C^{\text{sum}} \quad (36)$$

- linear fit to $S(t)$ yields g_A^{sum}
- still a systematic dependence on t_c

Backup – Summation method

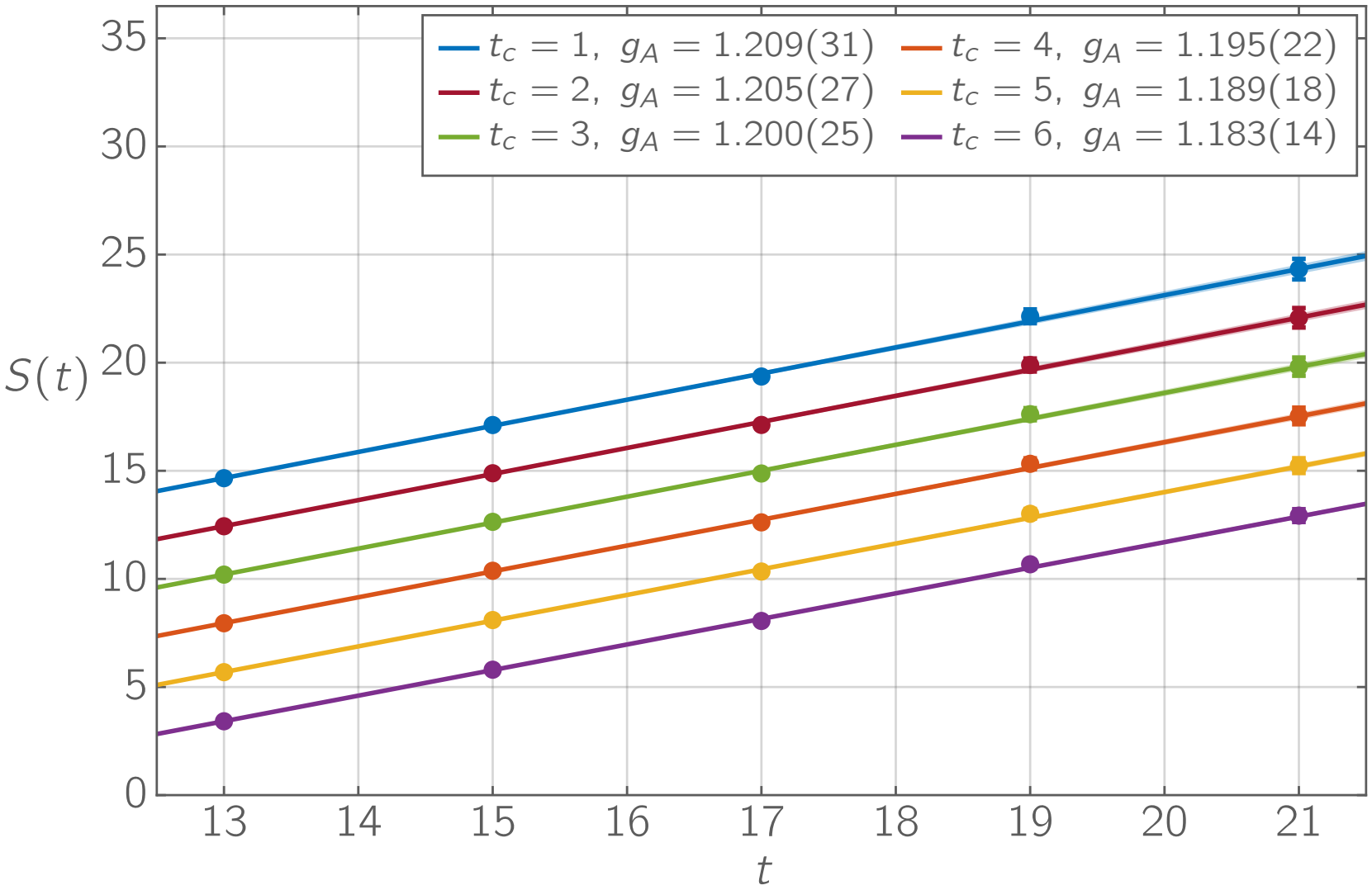

Figure 15: Summation method fit for $\beta = 5.50$

Backup – Summation method

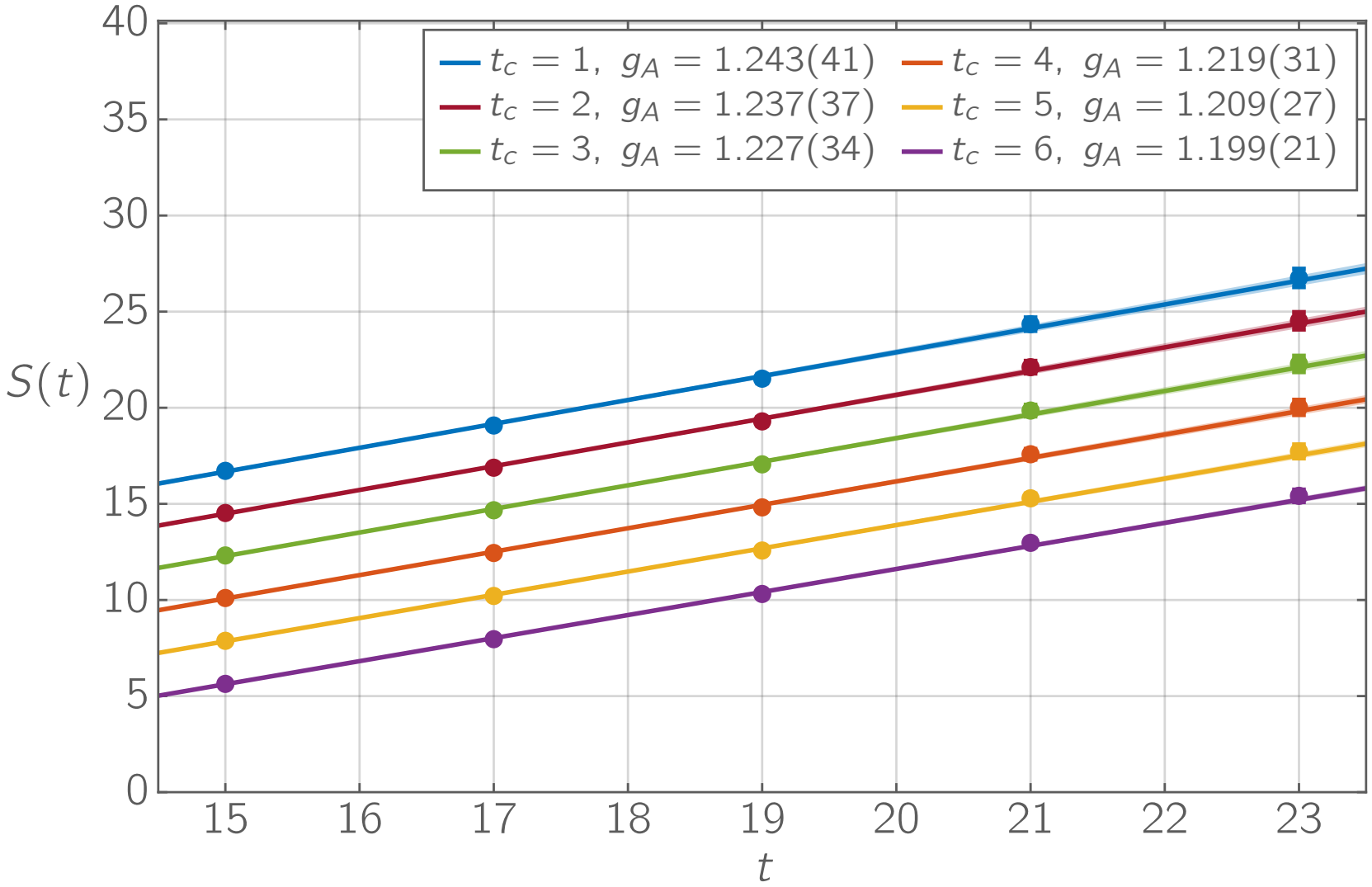

Figure 16: Summation method fit for $\beta = 5.80$

Backup – Feynman-Hellmann Approach

- additional effective term in the Lagrangian

$$L \to L + \lambda O \tag{37}$$

the theorem states for any hadron state H

$$\frac{\partial E}{\partial \lambda}|_{\lambda=0} = \frac{1}{2E}\langle H|O(0)|H\rangle \tag{38}$$

- measurement steps:
  1. perform hadron spectroscopy for multiple values of λ
  2. observe the linear behavior in the resulting energy shifts about $\lambda = 0$
- advantage: no three-point correlation functions needed and therefore less noticeable excited states contributions
- disadvantage: new configuration are needed for each operator and each λ

Backup – g_A summary

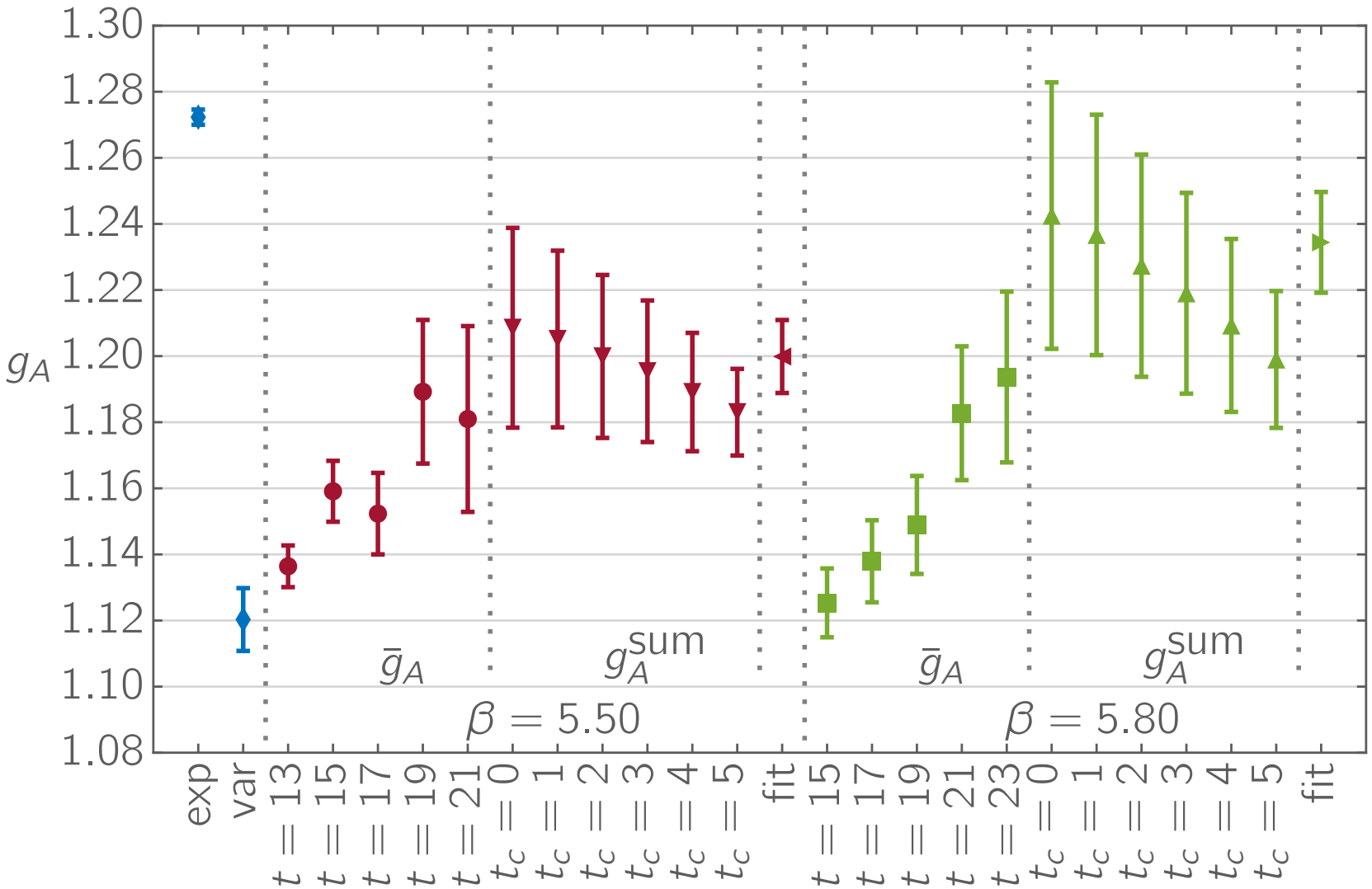

Figure 17: All obtained g_A values and reference values

Backup – g_A summary

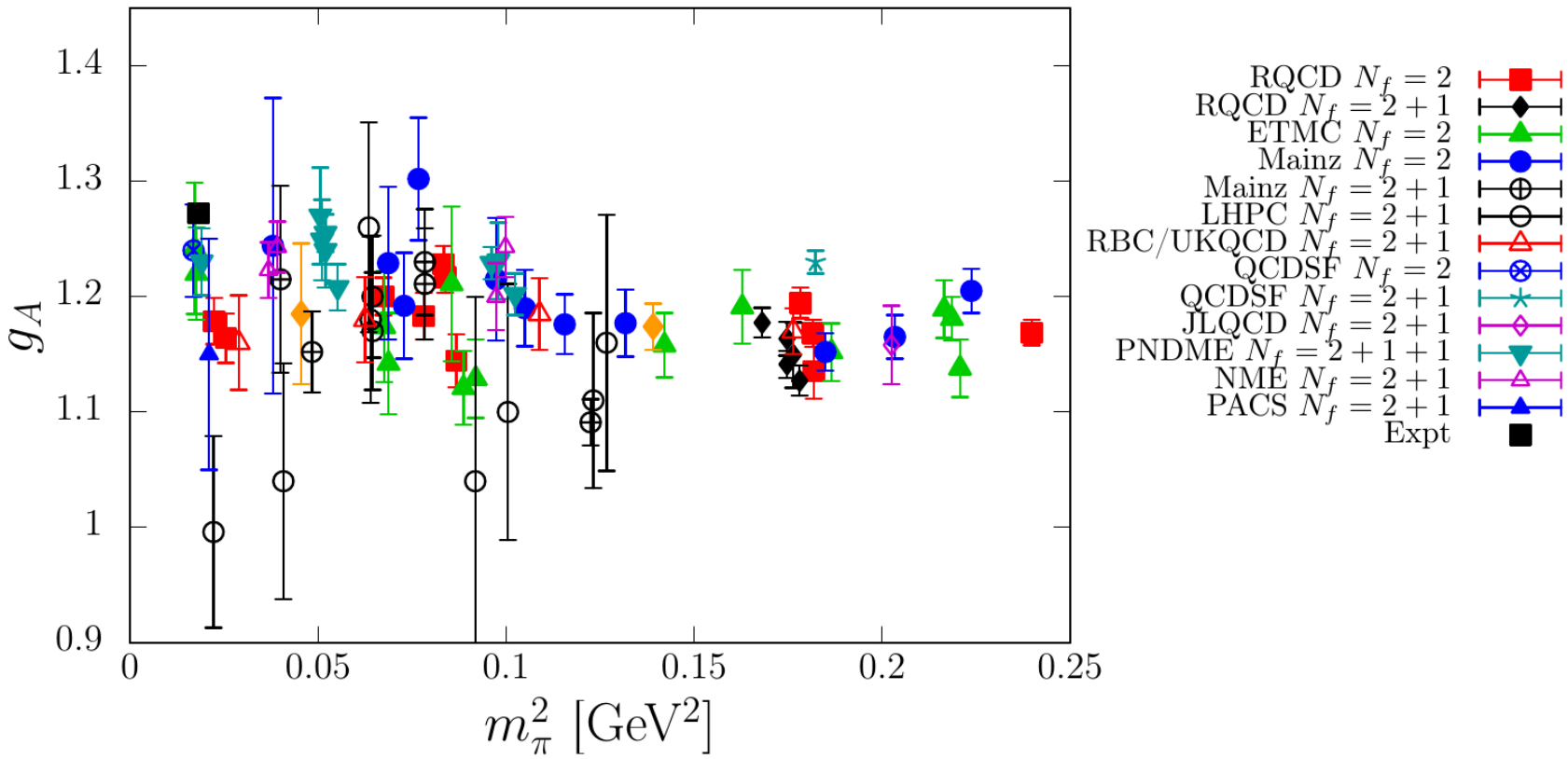

Figure 18: g_A measurements from different collaborations, point-split operator is used for "QCDSF $N_f = 2 + 1$"

Backup – RI'-MOM Scheme

consider a quark bilinear operator: $\mathcal{O}(z) = \bar{u}(z)\Gamma_{\mathcal{O}} d(z)$ (39)

- renormalization condition at a scale μ_R

$$Z_{\mathcal{O}} \frac{1}{12} \mathrm{Tr}\left(\langle u(p)|\mathcal{O}(z)|\bar{d}(p)\rangle \langle u(p)|\mathcal{O}(z)|\bar{d}(p)\rangle_0^{-1} \right) |_{\substack{p^2=\mu_R^2 \\ m\to 0}} = 1 \tag{40}$$

- scale window: $\Lambda_{QCD}^2 \ll \mu_R^2 \ll \frac{1}{a^2}$ (41)
- after some transformations and insertions

$$Z_{\mathcal{O}}(p) = \left. \frac{12\ Z_q(p)}{\mathrm{Tr}\left(\Lambda_{\mathcal{O}}(p) \Gamma_{\mathrm{B}}^{-1} \right)} \right|_{\substack{p^2=\mu_R^2 \\ m\to 0}} \tag{42}$$

$$Z_q(p) = \left. \frac{\mathrm{Tr}\left(-\mathrm{i} \sum_\mu \gamma_\mu \sin(a p_\mu) S^{-1}(p) \right)}{12 \sum_\mu \sin^2(a p_\mu)} \right|_{p^2=\mu_R^2} \tag{43}$$

Backup – RI'-MOM Scheme

- Born term is equal to the tree level matrix element

$$\langle u(p)|\mathcal{O}(z)|\bar{d}(p)\rangle_0 = \Gamma_{\mathrm{B}} \tag{44}$$

- amputated vertex function

$$\langle u(p)|\mathcal{O}(z)|\bar{d}(p)\rangle = Z_q^{-1}\Lambda_{\mathcal{O}}(p)\Lambda_{\mathcal{O}}(p) \quad = S^{-1}(p)\,G_{\mathcal{O}}(p)S^{-1}(p) \tag{45}$$

- propagator $S(p)$

$$S(p) = \int \mathrm{d}^4x \int \mathrm{d}^4y\; e^{-\mathrm{i}p(x-y)}S(x,y) \tag{46}$$

- vertex function $G_{\mathcal{O}}$

$$G_{\mathcal{O}}(p) = \frac{1}{V}\int \mathrm{d}^4x \int \mathrm{d}^4y \sum_z e^{-\mathrm{i}p(x-y)}\langle u(x)|\mathcal{O}(z)|\bar{d}(y)\rangle \tag{47}$$

Backup – RI'-MOM Scheme

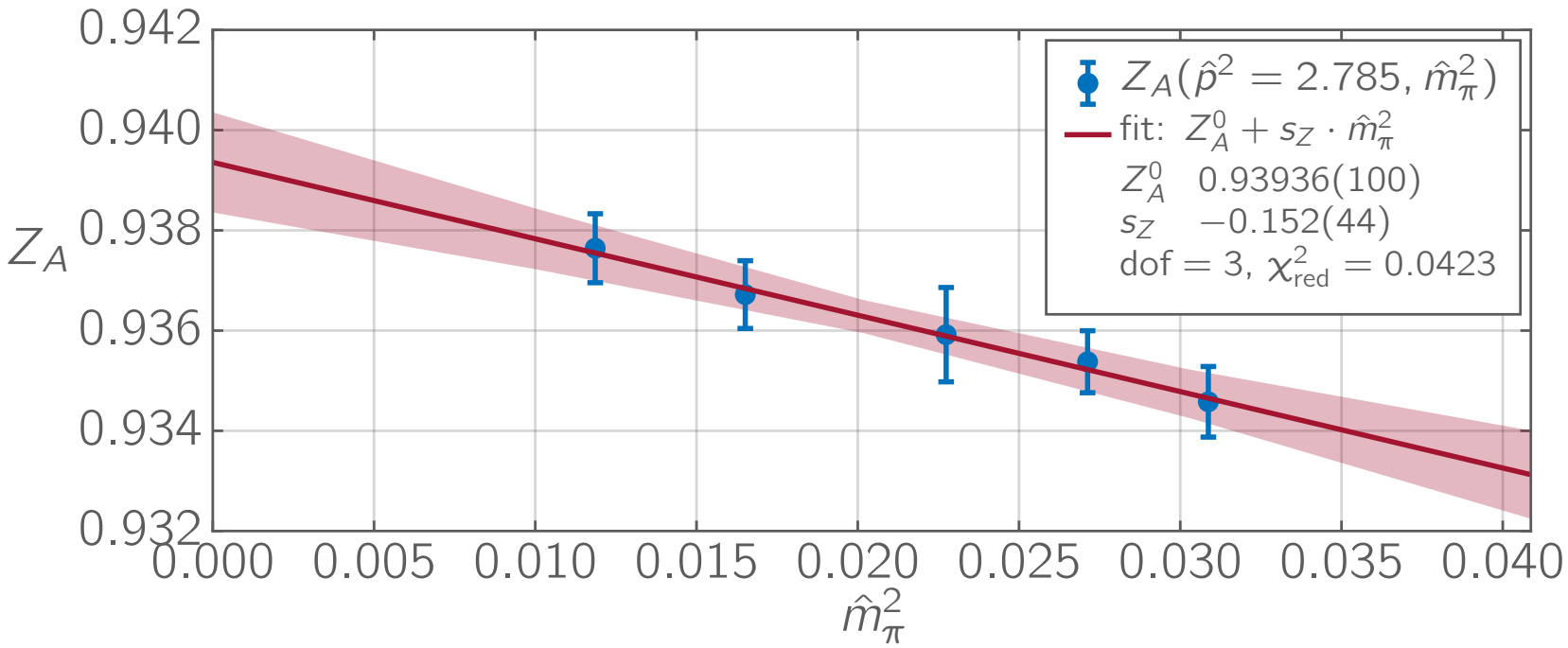

Figure 19: Chiral limit fit example

Backup – RI'-SMOM Scheme

- In RI'-MOM scheme:

$$p_1^2 = p_2^2 = \mu_R^2\,, \quad q = p_2 - p_1 = 0 \tag{48}$$

- exceptional channel where $q^2 \ll \mu_R^2$
- asymmetric subtraction point
- chiral symmetry breaking effects decrease as $1/p^2$
- In RI'-SMOM scheme:

$$p_1^2 = p_2^2 = q^2 = \mu_R^2\,, \quad q = p_2 - p_1 \neq 0 \tag{49}$$

- no exceptional channels
- symmetric subtraction point
- chiral symmetry breaking effects decrease as $1/p^6$
- some changes in the amputated vertex function are needed

Backup – Applications

Some applications of lattice QCD

- hadronic matrix elements
- confinement mechanism
- gluon self-interaction
- spontaneous chiral symmetry breaking
- ...

QCD action in continuum

$$S(A,\psi,\bar{\psi}) = \frac{1}{2g^2}\int \mathrm{d}^4x\ \mathrm{Tr}\left(F_{\mu\nu}(x)F_{\mu\nu}(x)\right) + \\ + \sum_f \int \mathrm{d}^4x\ \bar{\psi}_f(x)\left(\gamma_\mu D_\mu(x) + m_f\right)\psi_f(x) \qquad (50)$$

- fermion fields ψ_f and $\bar{\psi}_f$ with mass m_f and flavor index f
- gauge field A
- gauge coupling constant g
- field strength tensor $F_{\mu\nu}$
- covariant derivative D_μ

$$D_\mu(x) = \partial_\mu + \mathrm{i}A_\mu(x) \qquad (51)$$

Gauge fields $A_\mu(x)$

- represent the gluons
- elements of Lie algebra su(3)
- directional index μ
- $N_c^2 - 1$ ($= 8$ for $N_c = 3$) generators T^B of su(3)

$$A_\mu(x) = \sum_{B=1}^{8} A_\mu^B(x)\, T^B \tag{52}$$

- color components $A_\mu^B(x)$

Field strength tensor $F_{\mu\nu}(x)$

- commutator $[\, A_\mu(x)\,,\, A_\nu(x)\,]$ does not vanish

$$F_{\mu\nu}(x) = -\mathrm{i}[\, D_\mu(x)\,,\, D_\nu(x)\,] \tag{53}$$

$$F_{\mu\nu}(x) = \partial_\mu A_\nu(x) - \partial_\nu A_\mu(x) + \mathrm{i}[\, A_\mu(x)\,,\, A_\nu(x)\,] \tag{54}$$

- representation with generators and structure constants f^{ABC}

$$F_{\mu\nu}(x) = \sum_{B=1}^{8} F^B_{\mu\nu}(x)\, T^B \tag{55}$$

$$F^A_{\mu\nu}(x) = \partial_\mu A^A_\nu(x) - \partial_\nu A^A_\mu(x) - f^{ABC}\, A^B_\mu(x) A^C_\nu(x) \tag{56}$$

Fermion fields $\psi_f(x)$ and $\bar{\psi}_f(x)$

- live on lattice sites
- positional index $x \in \Lambda$
- physical spatial distance is ax

Note:

- all quantities are measured in lattice units a
- fermion fields, derivatives and masses are dimensionless

$$m \to am \tag{57}$$

$$\psi(x) \to a^{3/2}\psi(x) \tag{58}$$

$$\bar{\psi}(x) \to a^{3/2}\bar{\psi}(x) \tag{59}$$

Backup – Continuum QCD

Lattice derivative ∂_μ

forward-backward difference as derivative

$$\partial_\mu \psi(x) = \frac{1}{2} \left(\psi(x + \hat{\mu}) - \psi(x - \hat{\mu}) \right) \tag{60}$$

Covariant derivative $D_\mu(x)$

use link variables U_μ instead of gauge fields A_μ and discretize

$$D_\mu(x)\psi(x) = \frac{1}{2} \left(U_\mu(x)\psi(x + \hat{\mu}) - U_{-\mu}(x)\psi(x - \hat{\mu}) \right) \tag{61}$$

Wilson loop $U^{\square}(x)$

- closed loops of $U_\mu(x)$ are gauge invariant
- smallest closed loop is the Wilson loop

$$U^{\square}_{\mu\nu}(x) = U_\mu(x) U_\nu(x+\hat{\mu}) U^\dagger_\mu(x+\hat{\nu}) U^\dagger_\nu(x) \tag{62}$$

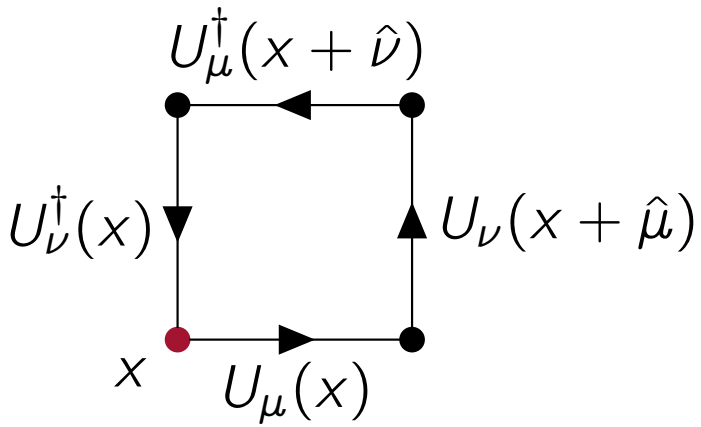

Figure 20: Wilson loop $U^{\square}_{\mu\nu}(x)$ starting at position x

Backup – Wilson QCD Action

Wilson gauge action $S_G^W(U)$

$$S_G^W(U) = \frac{\beta}{3} \int \mathrm{d}^4x \sum_{\mu<\nu} \mathrm{Re}\,\mathrm{Tr}\left(\mathbb{1} - U_{\mu\nu}^{\square}(x)\right) \tag{63}$$

Wilson fermion action $S_F^W(U, \psi, \bar{\psi})$

$$S_F^W(U, \psi, \bar{\psi}) = \sum_f \int \mathrm{d}^4x \int \mathrm{d}^4y \;\; \bar{\psi}_f(x)\, D_f^W(x, y)\, \psi_f(y) \tag{64}$$

- Wilson Dirac operator $D_f^W(x, y)$
- full lattice QCD Wilson action

$$S^W(U, \psi, \bar{\psi}) = S_F^W(U, \psi, \bar{\psi}) + S_G^W(U) \tag{65}$$

Backup – Wilson QCD Action

Wilson Dirac operator $D_f^W(x,y)$

- contains naive fermion action discretization and Wilson term
- Wilson term removes doublers from the action

$$D_f^W(x,y) = \mathbb{1}\delta_{xy} - \kappa_f \sum_\mu (\mathbb{1} - \gamma_\mu)\left(U_\mu(x)\delta_{x+\hat{\mu},y} - U_{-\mu}(x)\delta_{x-\hat{\mu},y}\right) \tag{66}$$

- Wilson action ready for calculations
- Wilson gauge action: $O(a^2)$ artifact effects
- Wilson fermion action: $O(a)$ artifact effects
- improvements useful

Backup – Action Improvements

Clover term

$$S_F^{SW}(U,\psi,\bar{\psi}) = -c_{SW}\sum_f \kappa_f \int \mathrm{d}^4x\, \bar{\psi}_f(x)\frac{1}{2}\sigma_{\mu\nu}\hat{F}_{\mu\nu}(x)\psi_f(x) \tag{67}$$

- improve fermion action to order $O(a^2)$
- improved action: $S_F = S_F^W + S_F^{SW}$
- clover coefficient c_{SW}
- matrices: $\sigma_{\mu\nu} = \frac{1}{2}[\,\gamma_\mu\,,\,\gamma_\nu\,]$ (68)
- field strength tensor on lattice $\hat{F}_{\mu\nu}(x)$

$$\hat{F}_{\mu\nu}(x) = \frac{1}{8}\left(Q_{\mu\nu}(x) - Q_{\nu\mu}(x)\right) \tag{69}$$

- $Q_{\mu\nu}(x)$ is a sum of plaquettes

$$Q_{\mu\nu}(x) = U^{\square}_{\mu,\nu}(x) + U^{\square}_{-\mu,\nu}(x) + U^{\square}_{\mu,-\nu}(x) + U^{\square}_{-\mu,-\nu}(x) \quad (70)$$

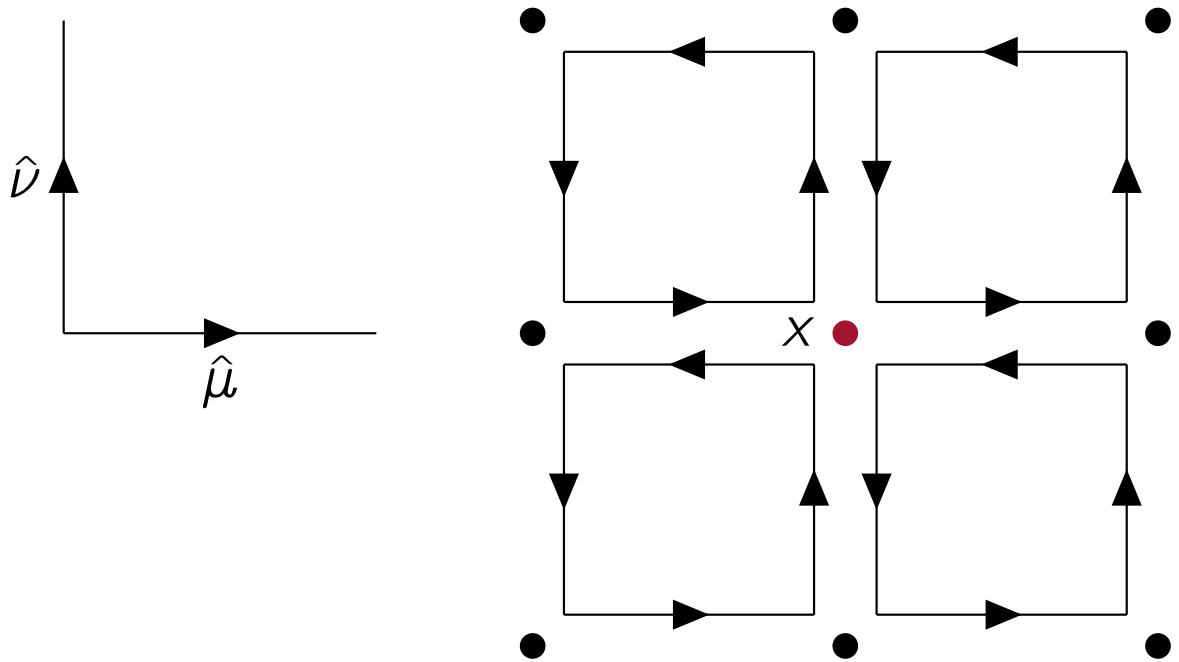

Figure 21: clover term $Q_{\mu\nu}(x)$ starting at position x

Backup – Action Improvements

Tree level Symanzik improved gauge action

$$S_G(U) = \frac{\beta}{3} \int \mathrm{d}^4 x \left(C_0 \sum_{\mu<\nu} \mathrm{Re}\,\mathrm{Tr} \left(\mathbb{1} - U^{\square}_{\mu\nu}(x) \right) + \right.$$
$$\left. + C_1 \sum_{\mu<\nu} \mathrm{Re}\,\mathrm{Tr} \left(\mathbb{1} - R^{\square}_{\mu\nu}(x) \right) \right) \qquad (71)$$

- include planar rectangles $R^{\square}_{\mu\nu}(x)$
- constants depend on each other $C_0 = 1 - 8C_1$
- in tree-level Symanzik improvement $C_1 = -\frac{1}{12}$
- possible to cancel order $O(a^2)$ artifacts and stay with $O(a^4)$

Backup – Action Improvements

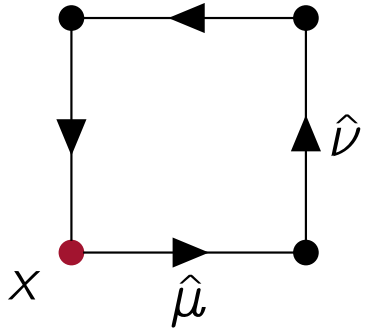

a plaquette $U^{\square}(x)$

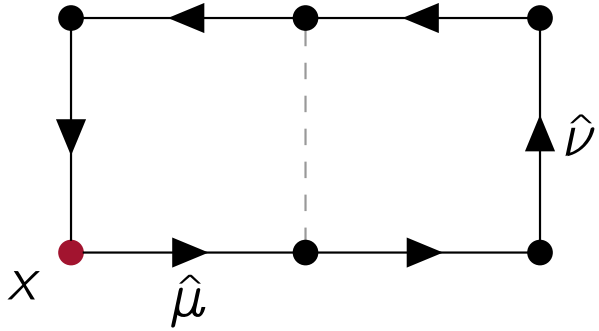

b planar rectangle $R^{\square}_{\mu\nu}(x)$

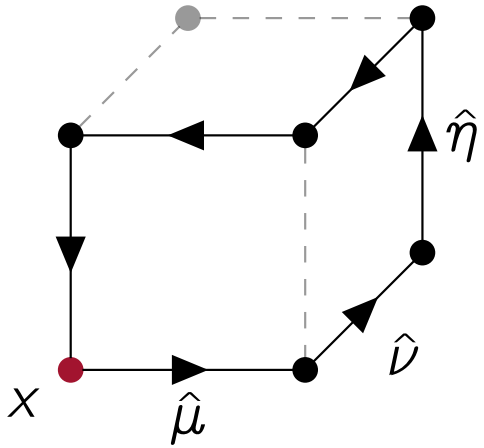

c extended rectangle $R^{\square}_{\mu\nu\eta}(x)$

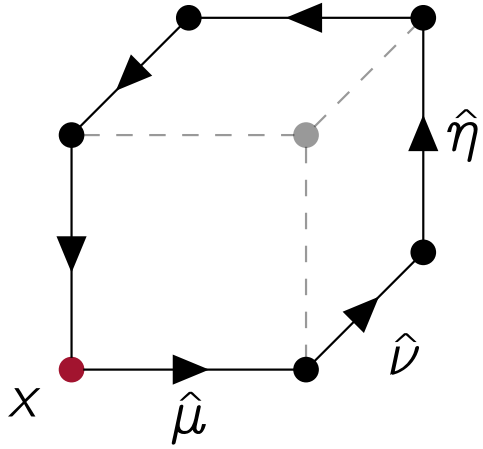

d extended bent rectangle $\tilde{R}^{\square}_{\mu\nu\eta}(x)$

Figure 22: schematic Wilson loop $U^{\square}(x)$ and rectangles $R^{\square}(x)$

Backup – Final QCD Action

$$S(U,\psi,\bar{\psi}) = S_F(U,\psi,\bar{\psi}) + S_G(U) \tag{72}$$

$$S_G(U) = \frac{\beta}{3}\int \mathrm{d}^4x \left(C_0 \sum_{\mu<\nu} \mathrm{Re\,Tr}\,\left(\mathbb{1} - U^{\square}_{\mu\nu}(x)\right) + \right.$$
$$\left. + C_1 \sum_{\mu<\nu} \mathrm{Re\,Tr}\,\left(\mathbb{1} - R^{\square}_{\mu\nu}(x)\right) \right) \tag{73}$$

$$S_F(U,\psi,\bar{\psi}) = \sum_f \int \mathrm{d}^4x \int \mathrm{d}^4y \;\; \bar{\psi}_f(x) D_f(x,y) \psi_f(y) \tag{74}$$

$$D_f(x,y) = \mathbb{1}\delta_{xy} - \kappa_f \sum_{\mu} (\mathbb{1} - \gamma_\mu)\left(U_\mu(x)\delta_{x+\hat{\mu},y} - U_{-\mu}(x)\delta_{x-\hat{\mu},y}\right) -$$
$$- c_{SW}\kappa_f \sum_{\mu,\nu} \frac{1}{2}\sigma_{\mu\nu}\hat{F}_{\mu\nu}(x)\delta_{xy} \tag{75}$$

Backup – Expectation Values

Expectation value of operator $\mathcal{O}$

- path integral formalism
- definition as in continuum

$$\langle \mathcal{O} \rangle = \frac{1}{\mathcal{Z}} \int \mathcal{D}U \, \mathcal{D}\psi \, \mathcal{D}\bar{\psi} \, \mathcal{O}(U, \psi, \bar{\psi}) \, e^{-S(U,\psi,\bar{\psi})} \tag{76}$$

- partition function $\mathcal{Z}$

$$\mathcal{Z} = \langle \mathbb{1} \rangle = \int \mathcal{D}U \, \mathcal{D}\psi \, \mathcal{D}\bar{\psi} \, e^{-S(U,\psi,\bar{\psi})} \tag{77}$$

measures:

$$\mathcal{D}\psi \, \mathcal{D}\bar{\psi} = \prod_{x \in \Lambda} \prod_{f,\alpha,c} \mathrm{d}\psi_f(x)^c_\alpha \mathrm{d}\bar{\psi}_f(x)^c_\alpha \, , \; \mathcal{D}U = \prod_{x \in \Lambda} \prod_{\mu} \mathrm{d}U_\mu(x) \tag{78}$$

Backup – Expectation Values

- Grassmann numbers (anti-commuting numbers) allow to integrate out the fermionic part

$$\langle \mathcal{O} \rangle = \frac{1}{\mathcal{Z}} \int \mathcal{D}U \prod_f \det D_f(x,y)\, \tilde{\mathcal{O}}(S_f, U)\, e^{-S_G(U)} \tag{79}$$

$$\mathcal{Z} = \int \mathcal{D}U \prod_f \det D_f(x,y)\, e^{-S_G(U)} \,. \tag{80}$$

- in $\tilde{\mathcal{O}}$ fermionic part was integrated out
- $\tilde{\mathcal{O}}$ depends only on link variables and quark propagators

Quark propagator $S_f(x,y)$

$$S_f(x,y) = D_f^{-1}(x,y) = \langle \psi_f(x) \bar{\psi}_f(y) \rangle_F \tag{81}$$

Backup – Expectation Values

- integral $\int \mathcal{D}U$ very high dimensional
- use Monte Carlo techniques for calculation
- have to deal with the fermion determinant

Fermion determinant $\det D_f(x, y)$

1. simplest solution – quenched approximation: $\det D_f = 1$
2. treat as an effective action and add to the gluon action

$$S_F^{\text{eff}}(U) = -\sum_f \operatorname{Tr} \ln D_f \prod_f \det D_f = e^{-S_F^{\text{eff}}} \tag{82}$$

$$\tilde{S}(U) = S_G(U) + S_F^{\text{eff}}(U) \tag{83}$$

3. other possibilities

Backup – Expectation Values

$$\langle \mathcal{O} \rangle = \frac{1}{\mathcal{Z}} \int \mathcal{D}U \; \mathcal{O} \; e^{-\tilde{S}(U)} \tag{84}$$

$$\mathcal{Z} = \int \mathcal{D}U \; e^{-\tilde{S}(U)} \tag{85}$$

this form calls for Monte Carlo technique

Monte Carlo basic simulation steps

1. configuration generation
2. operator measurement
3. data analysis

Backup – Configuration Generation

Configuration ensemble

configuration $\mathcal{U}_i$ is a set of link variables

$$\mathcal{U}_i = \{U_\mu(x) \mid x \in \Lambda,\ \mu = 1, \ldots, 4\} \tag{86}$$

ensemble $\mathcal{U}$ is a set of N_{cfg} configurations $\mathcal{U}_i$

- generate configuration ensemble $\mathcal{U}$
- configurations $\mathcal{U}_i$ distributed according to the weight

$$W = \frac{1}{\mathcal{Z}}\ e^{-\tilde{S}(U)} \tag{87}$$

- main difficulty:
  - local link updates: many updates needed to uncorrelate
  - global updates: low acceptance rate
  - possible solution: Hybrid Monte Carlo algorithm

Backup – Configuration Generation

Hybrid Monte Carlo algorithm

- idea: do a step from $\mathcal{U}$ to $\mathcal{U}'$ by performing a Hamiltonian molecular dynamics in fictitious time
- use concept of pseudofermions

Basic steps:

1. start with configuration $\mathcal{U}$
2. generate momenta p
3. evaluate the Hamiltonian $\mathcal{H}(\mathcal{U}, p)$
4. perform molecular dynamic in fictitious time $t \rightarrow \mathcal{U}', p'$
5. evaluate the Hamiltonian $\mathcal{H}'(\mathcal{U}', p')$
6. accept $\mathcal{U}'$ according to Metropolis probability

$$P = \min(1, e^{\mathcal{H}(\mathcal{U},p)-\mathcal{H}'(\mathcal{U}',p')})$$

7. if accepted: $\mathcal{U} := \mathcal{U}'$ an go to 1

Backup – Measurement

Importance sampling

- generated configurations $\mathcal{U}_i$ are distributed with $\frac{1}{\mathcal{Z}}\, e^{-\tilde{S}(U)}$
- expectation value estimator: $\langle \mathcal{O} \rangle = \frac{1}{N_{\text{cfg}}} \sum_{i=1}^{N_{\text{cfg}}} \mathcal{O}_i$ (88)
- standard error: $\sigma_{\bar{\mathcal{O}}} = \sqrt{\frac{\langle \mathcal{O}^2 \rangle - \langle \mathcal{O} \rangle^2}{N_{\text{cfg}}(N_{\text{cfg}} - 1)}}$ (89)
- often need bootstrap or jackknife method to obtain errors

use operators as two or three point correlators e.g. pion two point correlation function with pion interpolator $P(x) = \bar{d}(x)\gamma_5 u(x)$

$$\mathcal{O} = \langle P(x)\bar{P}(y) \rangle_F = \text{Tr}\left(\gamma_5 S_u(x,y)\gamma_5 S_d(y,x)\right) \quad (90)$$